TECHNICAL REPORT M-70-14

PENETRATION RESISTANCE OF SOILS

Report 2

GAMMA-RAY TECHNIQUES FOR NONDESTRUCTIVE MEASUREMENTS OF SOIL DENSITY AND DENSITY PROFILE

by

A. N. Williamson, Jr.

November 1970

Destroy this report when no longer needed. Do not return
it to the originator.

PENETRATION RESISTANCE OF SOILS

Report 2

GAMMA-RAY TECHNIQUES FOR NONDESTRUCTIVE MEASUREMENTS OF SOIL DENSITY AND DENSITY PROFILE

by

A. N. Williamson, Jr.

FOREWORD

The study reported herein constitutes a portion of the test program conducted during the period 1966-1968 and funded by Project 4A013001A91D, "In-House Laboratory Initiated Research Program," Item S, sponsored by the Assistant Secretary of the Army (R&D).

The tests were conducted by personnel of the former Remote Sensing Section (RSS) of the Mobility and Environmental (M&E) Division, U. S. Army Engineer Waterways Experiment Station (WES), under the general supervision of Messrs. W. G. Shockley and S. J. Knight, Chief and Assistant Chief, respectively, M&E Division, and Dr. D. R. Freitag, former Chief, Mobility Research Branch (MRB), now Chief, Office of Technical Programs and Plans, WES. Mr. B. R. Davis, former Chief, RSS, directed the study with the assistance of Dr. H. Nikodem and Mr. A. N. Williamson. This report was written by Mr. Williamson.

Acknowledgment is made of the cooperation and assistance provided by Mr. A. J. Green, Research Projects Group, MRB, and by other MRB staff members, who were responsible for sample preparation and other portions of the test program.

COL John R. Oswalt, Jr., CE, COL Levi A. Brown, CE, and COL Ernest D. Peixotto, CE, were Directors of the WES during the investigation and preparation of this report. Messrs. J. B. Tiffany and F. R. Brown were Technical Directors.

CONTENTS

NOTATION

C_r — Channel location of Co^{60} photopeak in reference spectrum

C_s — Channel location of Co^{60} photopeak in soil spectrum

D — Center-to-center distance from source to detector, cm

D_o — Unity center-to-center distance from source to detector, cm

D_r — Center-to-center distance from source to detector for reference measurements, cm

D_s — Center-to-center distance from source to detector for measurements on soil, cm

D_1 — A given center-to-center distance from source to detector, cm

D_2 — A center-to-center distance from source to detector greater than D_1, cm

e — Base of Naperian logarithm (2.71828)

E — Initial photon energy, Mev

E' — Energy of scattered photon, Mev

K_i — Average proportional change required in the vertical direction to achieve coincidence or near coincidence of soil and reference spectra

L_i — Average proportional change required in the horizontal direction to achieve coincidence or near coincidence of the soil and reference spectra

L_1 — Ratio of the channel location of the photon counts N_1 to the average channel location of the photon counts for all reference measurements

L_2 — Ratio of the channel location of the photon counts N_2 to the average channel location of the photon counts for all reference measurements

N	Number of photon counts detected per unit time from a radioactive source
N_b	Number of background counts
N_o	Number of photon counts detected per unit time from a source placed a unit distance from the detector
N_r	Number of photon counts within a certain energy range detected per unit time for reference measurements
N_s	Number of photon counts within a certain energy range detected per unit time for soil measurements
N_{s+b}	Total number of counts from Co^{60} source and background
N_1	Number of photon counts for a given thickness
N_2	Number of photon counts for an increase in thickness
R	Layer thickness affecting gamma-ray measurement, cm
x	Thickness of attenuating material, cm
$x_{\alpha l}$	Thickness of aluminum, cm
x_r	Thickness of reference material, cm
x_s	Thickness of soil, cm
x_w	Thickness of wood, cm
η	Mass attenuation coefficient, cm^2/g
$\eta_{\alpha l}$	Mass attenuation coefficient of aluminum, cm^2/g
η_r	Mass attenuation coefficient of reference material, cm^2/g
η_s	Mass attenuation coefficient of soil, cm^2/g
η_w	Mass attenuation coefficient of wood, cm^2/g
θ	Scattering angle, deg
ρ	Density of attenuating material, g/cm^3
$\rho_{\alpha l}$	Density of aluminum, g/cm^3
ρ_p	Predicted density, g/cm^3
$\rho_{p(\%)}$	Error in predicted density, percent
ρ_r	Density of reference material, g/cm^3
ρ_s	Density of soil, g/cm^3
ρ_w	Density of wood, g/cm^3
σ	Standard deviation

CONVERSION FACTORS, METRIC TO BRITISH UNITS OF MEASUREMENT

Metric units of measurement used in this report can be converted to British units as follows:

Multiply	By	To Obtain
centimeters	0.3937	inches
millimeters	0.03937	inches
square centimeters	0.155	square inches
cubic centimeters	0.061	cubic inches
meters	3.2808	feet
grams	0.0022	pounds
grams per cubic centimeter	62.43	pounds per cubic foot

SUMMARY

A study was conducted to determine the feasibility of using measurements made with a multichannel gamma-ray spectrometer and a cobalt 60 radiation source for accurately determining soil density and resolving the density profile of layers. Measurements were first made on aluminum and steel plates to establish a standard reference for computing soil density. Two samples of air-dry sand were constructed at different densities to depths of approximately 120 and 125 cm in a pit 51.82 m long and 3.54 m wide. Measurements were made at depth intervals of 12.7 cm in each of six access holes located in the samples. The densities determined were compared with densities determined by nonnuclear means.

Results of this study indicate that density can be measured accurately by the method described herein provided (a) the thickness through which the measurements are made is accurately measured, and (b) the source strength and detector are suitable for the distance over which the density is measured. The combination of source and detector that was used permitted defining soil density profiles.

As a result of this study, it is recommended that the method described herein be used for nondestructive soil density measurements where the density beneath the surface of a sample must be known.

PENETRATION RESISTANCE OF SOILS

GAMMA-RAY TECHNIQUES FOR NONDESTRUCTIVE MEASUREMENTS OF SOIL DENSITY AND DENSITY PROFILE

PART I: INTRODUCTION

Background

1. Rapid determination of soil moisture and soil density, particularly under field conditions where laboratory equipment is minimal, has presented a challenge to soils engineers for many years. Therefore, the announcement by the Civil Aeronautics Administration (CAA) in 1950[1] of the development of nuclear equipment for measuring soil moisture and density stimulated considerable interest among soils engineers.

2. The U. S. Army Engineer Waterways Experiment Station (WES) reported evaluation of this nuclear equipment as early as 1955.[2] It was found to be costly, unreliable, and not particularly rapid.

3. The instruments were subsequently modified and evaluated in field tests reported by the CAA.[3,4] A second investigation was then conducted at the WES[5] to determine the suitability of the modified nuclear equipment for measuring moistures and densities of airfield base courses and subgrades. Particular consideration was given to the reliability and durability of the equipment and the accuracy of the measurements. It was determined that the probes used with this equipment were not adaptable to airfield studies because the measurements were still time-consuming and the density measurements were still not as accurate as those obtained by direct sampling methods.

4. There followed other studies in which laboratory and field measurements were made with nuclear instruments of various descriptions. However, it was not until 1960 that a report recorded satisfactory tests in which this type of instrumentation was used to monitor compaction on airfield pavement construction.[6] In that study, three surface probes were used to make in situ moisture and density measurements. The accuracy was

1

BLANK PAGE

sufficient for controlling compaction, and the time required for determining the moisture and density of sand was reduced one-third.

5. Sensors evaluated in studies discussed thus far contained a detector and a source of gamma radiation in one assembly. The source was separated from the detector by a lead shield so that only scattered gamma rays could be detected. Since scattering of gamma rays is caused by collision of gamma-ray photons with electrons, placing the sensor adjacent to the soil allowed measurements of the electron density of the soil. A change in electron density of soil is closely related to a change in bulk or in situ density.

6. The techniques used in the latter studies, however, still were not completely satisfactory because the volume of soil contributing to the density measurements made in this manner could not be clearly defined since it was bulbous and varied in size with the moisture content and density of the soil. Furthermore, if the techniques used were modified to permit measurements with a sensor inserted into the soil rather than with a sensor resting on the surface, the measurements would be subject to error introduced by rearrangement of the soil during the insertion process.

Purpose and Scope

7. This study was conducted to investigate the feasibility of using measurements of direct gamma radiation for determining the density of large volumes of sand. Tests were conducted in two phases. In the first, measurements were made on aluminum and steel plates to establish a standard reference for computing soil density. In the second, measurements were made on two large samples of air-dry sand constructed to different densities. At six locations in each sample, measurements were made at various depths to obtain a profile of density within the sample.

8. During preparation of the samples, a limited number of density measurements were made by weighing a known volume of sand that had been removed. These measurements were subsequently compared with the gamma-ray density measurements made.

2

PART II: RATIONALE

9. The number of photon counts N_o that are detected per unit time
from a radioactive source placed a unit distance away from a detector de-
pends on the characteristics of the source and detector, the test geometry,
and background radiation. If the source is one with a relatively long half-
life, and the source and detector characteristics, the test geometry, and
background radiation remain unchanged, N_o may be assumed to be a constant.

10. When a material is placed between the source and detector. the
number of photon counts detected N becomes, according to Lambert's ab-
sorption law,

$$N = N_o \exp(-\eta\rho x)*$$ (1)

where N is the number of counts detected per unit time from a radioactive
source a unit distance away, and η , ρ , and x are, respectively, the
mass attenuation coefficient, density, and thickness of the material be-
tween the source and the detector.

11. The mass attenuation coefficient of a material varies as a func-
tion of the energy level of the source of radiation. However, if the
energy level of the source and the chemical composition of the material be-
tween the source and detector are known, the mass attenuation coefficient
of the material can be determined from published tables. The thickness of
the material can be measured directly. Thus, it would appear that the only
remaining unknown, the density, could be computed directly from measure-
ments of N and N_o .

12. Unfortunately, such a direct approach to the determination of
densities of materials is not practicable, because it is not always pos-
sible to keep the source at a unit distance, nor is it possible to main-
tain a constant N_o . Consequently, the approach that was taken in this
study was somewhat indirect.

___

* $\exp(-\eta\rho x) = e^{-\eta\rho x}$, where e is the base of the Naperian logarithm
(2.71828).

3

13. The effect of distance between the source and detector was easily handled, since the number of photon counts follows the inverse square law. Therefore, provided all other factors remain constant,

$$N_2 = \left(D_1^2 / D_2^2\right) N_1 \tag{2}$$

where D is the distance between the source and detector.

14. The main problem, that of maintaining a constant N_o, had to be handled in the following manner:

    <u>a</u>. A spectrum of the number of gamma-ray counts versus channel number (energy level) was measured for various thicknesses of a reference material, in this case aluminum and steel plates, placed between a gamma-ray source and detector. A measurement of the spectrum of the background radiation, made with the source removed from the test area, accompanied each measurement on the reference material. The background spectrum was subtracted from the spectrum for the reference material so that only radiation from the gamma-ray source would be considered in subsequent determinations.

    <u>b</u>. Spectra for soil between the source and detector were then obtained in a similar manner.

    <u>c</u>. The spectrum for the reference material that had counts most nearly the same as those measured through soil was compared with each of the soil spectra; and the average proportional change in the vertical direction K_i and the average proportional change in the horizontal direction L_i necessary to achieve coincidence or near coincidence of the two spectra were noted. By this technique, the number of counts N_s measured when soil was the attenuating material was equal to $K_i L_i N_r$, where N_r is the number of counts measured for aluminum and steel, the reference materials.

Thus, for unit distance D_o,

$$N_s = N_o \exp\left(-\eta_s \rho_s x_s\right) \tag{3}$$

4

and

$$N_r = N_o \exp\left(-\eta_r \rho_r x_r\right) \tag{4}$$

For distances other than unity, equation 2 yields

$$N_s = N_o\left(D_o/D_s\right)^2 \exp\left(-\eta_s \rho_s x_s\right) \tag{5}$$

and

$$N_r = N_o\left(D_o/D_r\right)^2 \exp\left(-\eta_r \rho_r x_r\right) \tag{6}$$

When equations 5 and 6 are substituted for N_s and N_r, respectively, in $N_s = K_i L_i N_r$ (paragraph 14c), then

$$N_o\left(D_o/D_s\right)^2 \exp\left(-\eta_s \rho_s x_s\right) = K_i L_i N_o \left(D_o/D_r\right)^2 \exp\left(-\eta_r \rho_r x_r\right) \tag{7}$$

or

$$\exp\left(-\eta_s \rho_s x_s\right) = K_i L_i \left(D_s/D_r\right)^2 \exp\left(-\eta_r \rho_r x_r\right) \tag{8}$$

15. With N_o thus eliminated, the soil density is

$$-\eta_s \rho_s x_s = \ln K_i L_i + 2 \ln\left(D_s/D_r\right) - \eta_r \rho_r x_r \tag{9}$$

or

$$\eta_s \rho_s x_s = \eta_r \rho_r x_r - \ln K_i L_i - 2 \ln\left(D_s/D_r\right) \tag{10}$$

and

$$\rho_s = \frac{1}{\eta_s x_s}\left[\eta_r \rho_r x_r - \ln K_i L_i + 2 \ln\left(D_r/D_s\right)\right] \tag{11}$$

5

Equipment

Gamma-ray spectrometer

16. The spectrometer used in these studies is a multichannel system
that counts the number of gamma-ray photons that are detected within a
known length of time and arranges the counts according to energy level.
Principal components of the system (fig. 1) are described briefly below;
detailed descriptions are given in reference 7.

17. Sodium iodide detector assembly. The sodium iodide (NaI) de-
tector assembly (fig. 1a) is composed of a cylindrically shaped NaI crystal,
12.7 cm* in diameter and 12.7 cm high, mounted in a sealed enclosure with
an optically coupled photomultiplier tube. When a gamma-ray photon strikes
the crystal, the photon's energy is converted to light, the intensity of
which is proportional to the energy level of the gamma ray. The crystal is
activated with thallium to ensure maximum conversion of energy to light.
The photomultiplier tube detects the intensity of this light and produces
an electrical pulse with an amplitude proportional to the intensity of the
light and, hence, the energy level of the gamma-ray photon.

18. Pulse-height analyzer. The pulse-height analyzer (fig. 1b) re-
ceives the electrical pulses from the detector and sorts them into magnetic
ferrite core memory storage channels on the basis of their amplitude. The
pulse-height analyzer has 400 storage channels, but only 200 of these were
used in this study. The term "channel" refers to the location of the en-
ergy level band within the 200 channels used for accumulation of radiation
data in the pulse-height analyzer. Each channel will store the number of
pulses with energies over a range of 0.014168 Mev. Thus, from the bottom
of channel 1 to the top of channel 199, the number of detected pulses
stored will range in energy from 0 to 2.819 Mev. Channel 0 (zero) is used
to record the length of time during which counting has taken place (live
time). The pulse-height analyzer sorts and stores data for a preselected

* A table of factors for converting metric units of measurement to British
units is given on page xi.
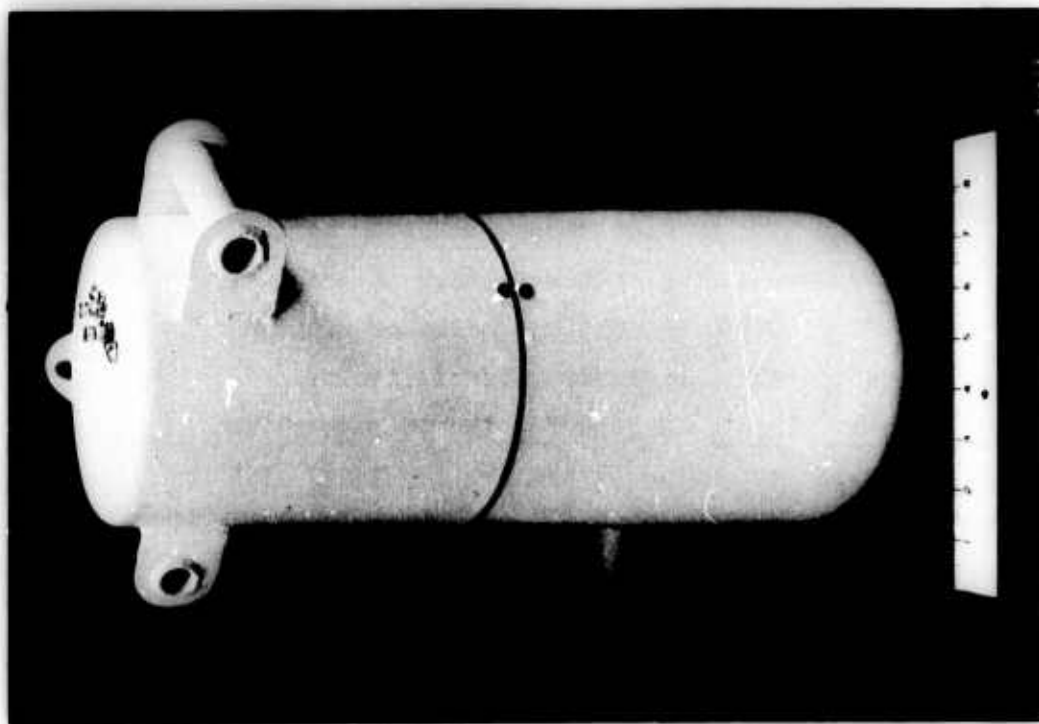
a. Sodium iodide detector assembly
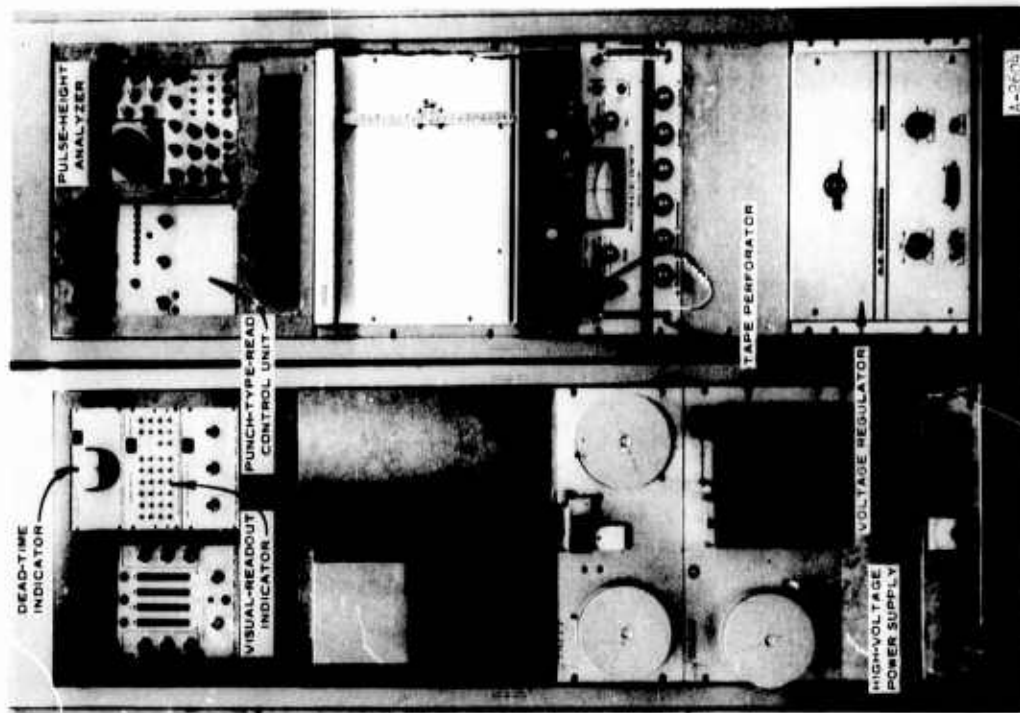
b. Cabinet-mounted components

Fig. 1. Gamma-ray spectrometer

period of live time, after which it ceases to accumulate additional data and either continues to store the data it has already accumulated or automatically releases the stored data to the paper-tape perforator.

19. Dead-time indicator. Each time the pulse-height analyzer accepts a signal from the detector, it is disabled for a short time during which it will not accept any additional input signals. During this period, called the dead time, the signal that has been accepted is sorted and stored in the proper channel according to signal amplitude. The dead-time indicator shows the percentage of the total time that is dead time, thereby providing an indication of the approximate photon flux at the detector.

20. Visual-readout indicator. After the pulse-height analyzer has stored all the information on the gamma-ray spectrum, the readout indicator provides the operator with a visual indication of the number of counts stored in each channel.

21. Punch-type-read control unit. The digital information from the pulse-height analyzer is converted to the proper format by the punch-type-read control unit to allow the stored data to be punched out on paper tape for computer analysis.

22. Paper-tape perforator. The paper-tape perforator receives information from the punch-type-read control unit and punches this information on paper tape along with a buzz code for leader control. The buzz code signal separates individual runs on a single tape.

23. High-voltage power supply. Precision voltage required for operation of the photomultiplier tube in the detector assembly is supplied by the high-voltage power supply. This voltage is precisely controlled to maintain a stability of 0.005 percent per hour, or 0.05 percent per day, and has a ripple component of less than 5.0 millivolts.

24. Voltage regulator. Except for the voltage to the high-voltage power supply, all voltages to the system are regulated with the line voltage regulator to an accuracy of 0.01 percent. This ensures proper functioning of the spectrometer with input voltage variations from 95 to 130 volts AC.

Radiation source

25. A 10-millicurie source of cobalt 60 was utilized in this study.

8

Co^{60} emits gamma radiation with an energy level of 1.33 Mev. Except during the short periods of time when it was being used for measurements, it was stored in a lead container with walls approximately 10 cm thick to reduce exposure of personnel to Co^{60} radiation to a minimum.

Apparatus for non-
nuclear density measurements

26. Samples for nonnuclear density measurements were taken with a gravimetric device consisting of a rectangular thin-walled box, two spoons, a scoop, a pan, and a brush (fig. 2). The box was open at the top and bottom and contained 1168.2 cm^3 of material when the height of the material in the box was 5.09 cm.
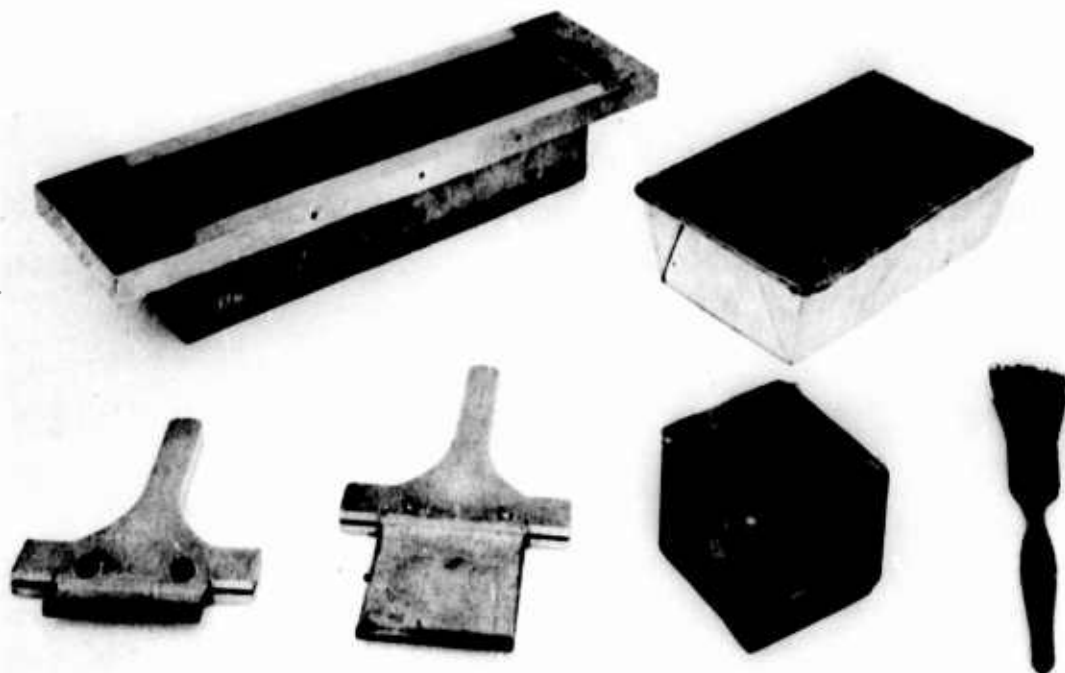

Fig. 2. Apparatus used to obtain sand samples
for density determinations

Test Program

27. The test program was divided into two phases. In the first phase, gamma-ray photons that passed from the Co^{60} source to the NaI crystal detector through materials of known physical properties were measured

to establish a reference for measurements on soils. In the second phase, measurements were made on two samples of air-dry Yuma sand that were constructed to different densities. The data from these measurements permitted computation of the mean density of horizontal layers of soil located between the source and the detector.

First phase

28. The first phase of the test program consisted of establishing the relation between the spectrum of gamma-ray counts versus channel number (energy level) for a reference material, and the mass attenuation coefficient, density, and thickness of that material.

29. Reference material. Reference spectra were measured on aluminum and steel plates, 3.8 cm thick and approximately 30.48 cm square, placed between the source and the detector. Aluminum plates were used because the plates and information on the physical properties of aluminum were readily available. The aluminum plates were augmented by a denser material, steel, because the total thickness of aluminum that could be measured, and thereby the range of measurements that could be defined, was limited by the distance separating the source from the detector. By comparing the number of gamma-ray counts transmitted through steel and aluminum plates, it was found that a 1-cm thickness of steel was equivalent to a 2.83-cm thickness of aluminum.

30. Measurement procedure. Reference measurements were made by sorting and storing gamma-ray counts with the pulse-height analyzer for a live time of 10 min. The Co^{60} source and the detector were separated by a distance of 159.7 cm. The source was surrounded on five of six sides with steel plates to form a shield with walls approximately 15 cm thick. The unshielded side provided a window through which the energy could be radiated in the direction of the detector. Extraneous radiation passing through the window of the shield was reduced to a minimum by placing the aluminum and steel reference plates in the space between the source and the detector so they would cover the window.

31. Radiation was first measured through a steel plate 16.4 cm thick (equivalent to an aluminum thickness of $16.4 \times 2.83 = 46.4$ cm). Subsequently, radiation was measured following the addition of each of three

3.8-cm-thick aluminum plates, to a total thickness equivalent to an aluminum thickness of 57.8 cm. The three aluminum plates were then replaced by a 3.8-cm-thick steel plate, and radiation was measured. The thickness of the two steel plates was equivalent to an aluminum thickness of 57.1 cm. With the steel plates remaining in position, subsequent measurements were made following the addition of each of five 3.8-cm-thick aluminum plates, to a total thickness equivalent to an aluminum thickness of 76.1 cm.

32. Each measurement of radiation through the reference plates was accompanied by a measurement of background radiation taken for a 10-min live time with the source removed from the test area.

Second phase

33. <u>Soil tested.</u> In the second phase, radiation was measured through two samples of Yuma sand, each constructed to a uniform density and moisture content. The first sample was prepared to a lower density than the second, so that the ability to distinguish different densities by gamma-ray measurements could be assessed. Yuma sand is a wind-sorted fine sand containing predominantly quartz. The particle sizes are nearly uniform, with 95 percent of the particles being between 0.07 and 0.30 mm in diameter. All of the particles are between 0.06 and 0.5 mm in diameter. A gradation curve and classification according to the Unified Soil Classification System appear in fig. 3. Sand used in these tests was obtained from stockpiles located at the WES. Prior to use, it was divested of roots and other foreign material and air dried to a moisture content of approximately 0.5 percent.

34. <u>Sample preparation.</u> Samples were prepared in a concrete pit located in the Mobility Research Branch (MRB) large-scale test facility. The pit is 51.82 m long, 3.54 m wide, and 1.68 m deep, with tracks down each side to allow movement of test carts and instrument platforms down the length of the test area without disturbing the sample. The first sample was constructed to a height of 121.8 cm, and the second to a height of 124.5 cm from the bottom of the pit.

35. Sand was placed in the pit in thin layers with a spreader (fig. 4) designed to travel along the tracks and distribute the sand uniformly over the surface of the sample. The density of the sample was
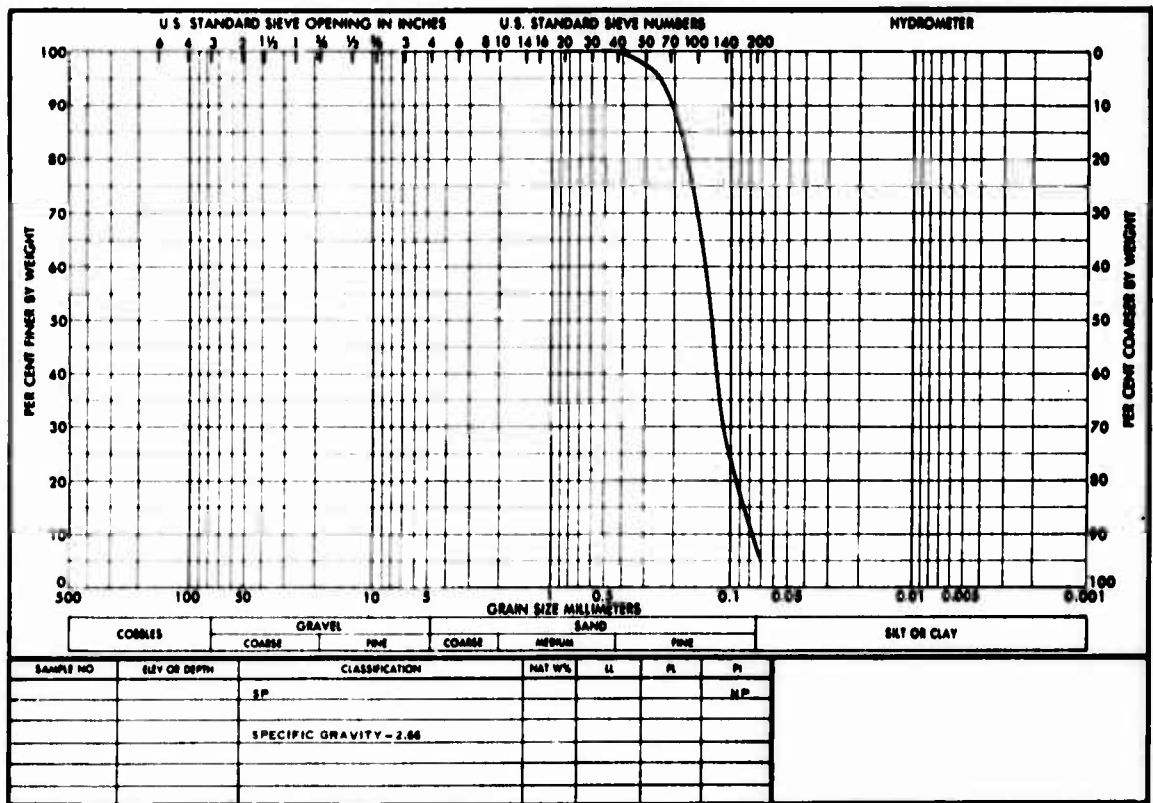
Fig. 3. Gradation curve for Yuma sand
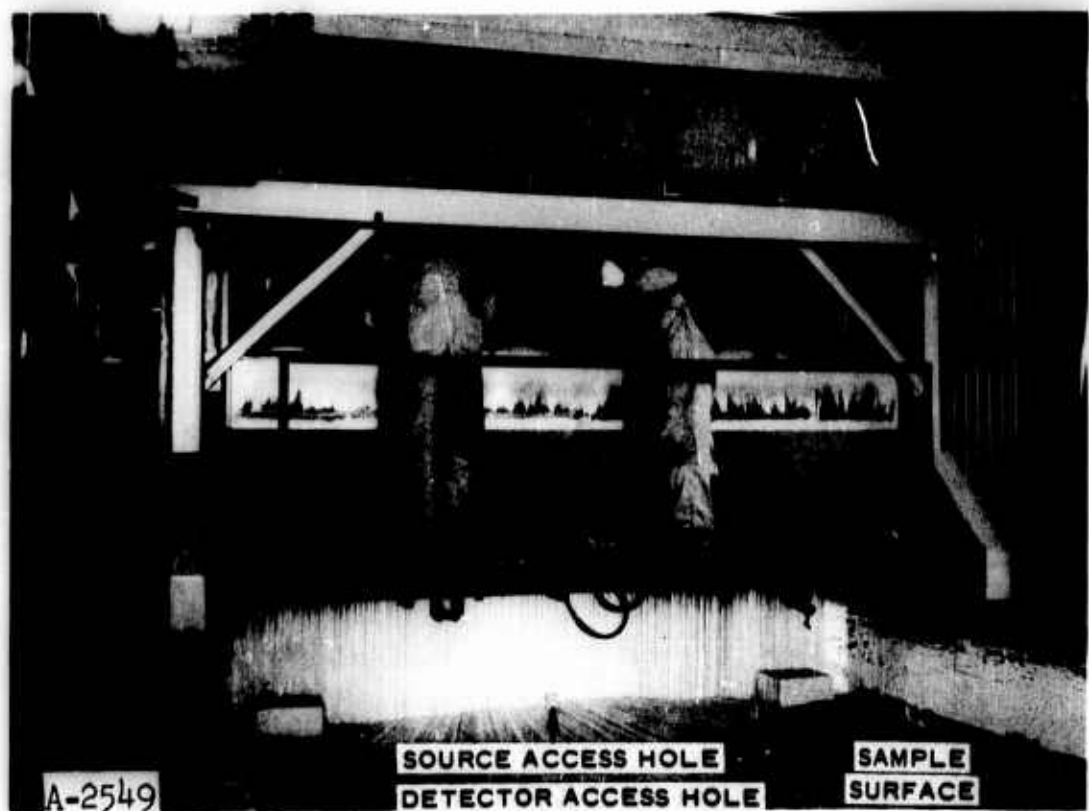
Fig. 4. Sand spreader

controlled by adjusting the rate of flow of the sand and the distance the
sand fell from the spreader to the top surface of the sample being con-
structed. A predetermined density could be obtained, provided the rate of
travel over the test pit was constant.

36. During preparation of a sample, access holes were formed in it
for the radioactive source and the detector. The holes for the source were
formed with aluminum tubes 7.6 cm in diameter and with walls 0.48 cm thick.
Wooden frames 30.5 cm square and with walls 1.3 cm thick were used to form
the access holes for the detector. The tubes and frames were in sections
15.2 cm long that could be joined by tongue-and-groove construction. As
the sand in the pit neared the top of the tubes and frames, sections were
joined until the final height of the sample to be tested was reached.

37. Prior to placement of the first layer of sand, sections of
tubes and frames were placed vertically in the pit at the locations shown
in fig. 5, with the tubes along the center line and the frames on opposite
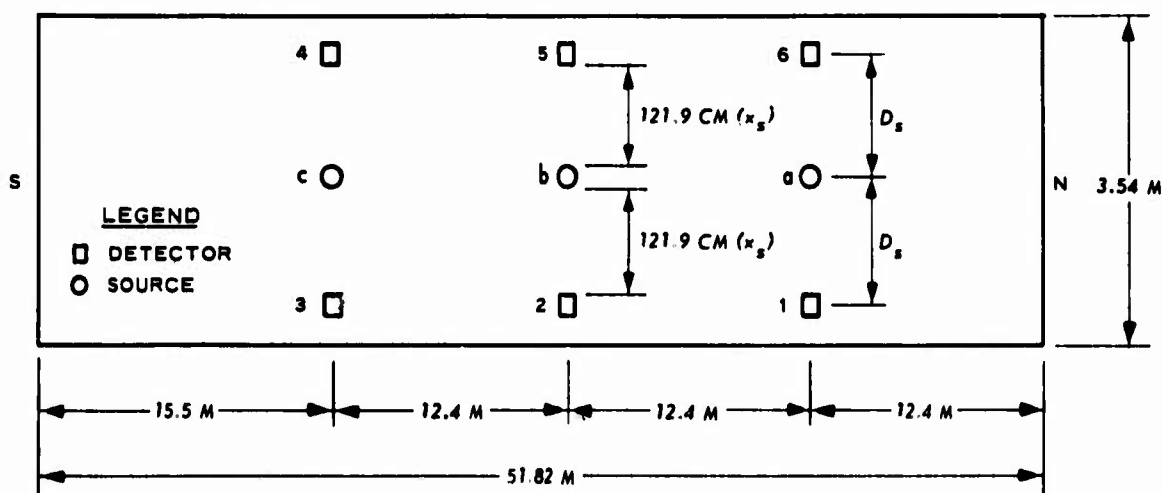
Fig. 5. Location of access holes

sides of the tubes. In this arrangement, a source access hole was common
to two detector access holes. The wooden frames were situated so the
thickness of sand between a frame and the aluminum tube was 121.9 cm. Dur-
ing preparation of the sample, the tubes and frames were temporarily covered
to prohibit sand from entering the access holes.

38. Nonnuclear density measurements. During construction of the
large samples of sand, a few small samples were taken from locations

13

adjacent to the detector access holes for determinations of density by conventional methods. The small samples were obtained by pushing the density box (fig. 2) into the sand until the lower surface of the collar of the box was in firm contact with the sand. At this point, the level of sand in the box was approximately 0.25 cm higher than the desired upper level and about 1.27 cm below the upper surface of the collar. The excess sand in the box was carefully removed to the desired level by using a short spoon designed so that the spoon cut the sand to the desired level when the shoulders of the spoon were in contact with the upper surface of the box. A scoop was then used to remove the sand remaining in the box to within 0.25 cm of the desired lower level. This sand was carefully placed in a pan. A spoon 41.8 cm longer than the first one was then used to remove the sand that remained in the box and convey it to the pan. Grains of sand that adhered to the scoop and long spoon were brushed into the pan. The known volume (1168.2 cm^3) of sand in the pan was then weighed and the density computed.

39. <u>Gamma-ray measurement technique.</u> For the gamma-ray measurements, the height of the source and the detector within the access holes had to be changed while a constant source-to-detector distance was maintained. This was accomplished by suspending the source and the detector from a movable beam positioned across the pit. Clamps attached to suspension cables facilitated prepositioning the source and the detector to the desired depths.

40. To define the gamma radiation passing through layers of soil, it was necessary to ensure that the source and the detector were accurately aligned in the same horizontal plane. This was done by positioning the radioactive source at the same elevation as the midpoint of the NaI crystal in the detector assembly. The NaI crystal was 12.7 cm high and was located in the bottom of the detector assembly. Therefore, optimum alignment of the source and the detector was achieved when the source was positioned in the access hole 6.35 cm higher than the bottom of the detector assembly. The initial measurements were made in each access hole with the bottom of the detector 6.4 cm from the bottom of the pit and that of the source 12.7 cm from the bottom of the pit. Subsequent measurements were made each time the source and detector were raised 12.7 cm.

41. Five layers were measured in sample No. 1. An initial measurement was made of the first three 12.7-cm layers with the sample constructed to an average height of 51.0 cm. After construction had progressed to a final height of 121.8 cm, measurements were repeated on these three layers and were made on two additional 12.7-cm layers above the original height of 51.0 cm.

42. After sample No. 2 had been constructed to an average height of 118.1 cm, nine layers were measured at increments of 12.7 cm. A final layer was measured 6.4 cm above the level of the ninth measurement in four of the six access holes. Because of a slight nonuniformity in the height of the sample on one end, the final measurements for holes 1 and 6 were made 7.6 cm above the ninth measurement. Dead times in excess of 15 percent, which indicated that excessive radiation was impinging on the detector, prohibited measurements any nearer the top surface of the soil samples.

43. <u>Test procedure.</u> Two gamma-ray measurements, each for a 10-min live time, were made at each detector and source height. One was a background measurement made with the detector suspended at the desired height in the access hole, but with the Co^{60} source removed from the test area. The other was similar to the first in all respects, except it was made with the source placed in its access hole at a height that would position it at the same elevation as the midpoint of the NaI crystal (paragraph 40).

PART IV: REDUCTION AND ANALYSIS OF DATA

Data Reduction

Spectra correction

44. <u>Gain and base-line shift.</u> The output of the gamma-ray spectrometer was a spectrum of the number of photon counts accumulated during a measurement of preset 10-min live time versus channel number. Each channel contained an energy range of 0.014168 Mev so that the peak counts for Co^{60}, which has an energy of 1.33 Mev, were normally located in channel 93.9 (1.33 ÷ 0.014168 = 93.9). However, instrumentation variations in gain and base line caused the peak to shift to adjacent channels. For this reason, the spectra measured on the sand samples were corrected with a computer program[7] designed to relocate the counts in their proper channels.

45. The computer program was written for measurements taken for a 100-min live time and the measurements in this study were taken for a 10-min live time. Thus, the output of the computer program was 10 times the number of counts measured in each channel. Since the reference measurements were not computer corrected, they had to be multiplied by 10 for comparison with the various soil measurements.

46. <u>Background radiation.</u> The gamma-ray spectra of the radiation from the Co^{60} source were records of the photon counts not only from the radioactive source, but also from all other sources of radioactivity that constituted the background. The background counts were found to vary over a wide range, so that it was desirable to minimize their contribution prior to analysis of the data. This was accomplished by subtracting the number of counts of the background spectrum in each channel between channel 90 and channel 100 from the number of counts in the corresponding channel of the spectrum measured with the radioactive source. The channels between 90 and 100 were used because the peak counts for Co^{60} were always contained within these limits, regardless of spectrum shifts due to gain and base-line variations.

Method for computing sand density ρ_s

47. Since aluminum tubes and wooden boxes were used to form holes in

16

the samples for access to the source and the detector, gamma radiation from the source was attenuated by the aluminum and wood as well as by the soil prior to reaching the detector. If the mass attenuation coefficient, density, and thickness of the wood are expressed as η_w, ρ_w, and x_w and the mass attenuation coefficient, density, and thickness of the aluminum as η_{al}, ρ_{al}, and x_{al}, equation 8 can be written:

$$\exp\left(-\eta_s\rho_s x_s - \eta_w\rho_w x_w - \eta_{al}\rho_{al}x_{al}\right) = K_1 L_1 \left(D_s/D_r\right)^2 \exp\left(-\eta_r\rho_r x_r\right) \quad (12)$$

to include the additional attenuation of aluminum and wood. Then

$$-\eta_s\rho_s x_s - \eta_{al}\rho_{al}x_{al} - \eta_w\rho_w x_w = -\eta_r\rho_r x_r + \ln\left(K_1 L_1\right) + 2\ln\left(D_s/D_r\right) \quad (13)$$

and

$$\rho_s = \frac{1}{\eta_s x_s}\left[-\eta_{al}\rho_{al}x_{al} - \eta_w\rho_w x_w + \eta_r\rho_r x_r - \ln\left(K_1 L_1\right) + 2\ln\left(D_r/D_s\right)\right] \quad (14)$$

48. The terms η_r, η_{al}, η_s, η_w, ρ_r, ρ_{al}, ρ_w, x_{al}, x_w, x_r, and D_r in equation 14 remained constant for all measurements in this study, while D_s, x_s, K_1, and L_1 could differ for each measurement. The methods used to determine the values for both the constant and variable terms are discussed in the paragraphs that follow.

49. <u>Determination of η_r</u>. The mass attenuation coefficient of the aluminum plates η_r was determined from measurements made in the first phase of this study. Each time a 3.8-cm-thick aluminum plate was placed between the source and detector, the Co^{60} counts diminished according to the equation

$$N_2 = N_1 \exp\left(-\eta_r\rho_r x_r\right) \quad (15)$$

where

N_1 = number of photon counts for a thickness of an attenuating material

N_2 = number of photon counts for an additional thickness x_r of the attenuating material

17

Since ρ_r and x_r were known ($\rho_r = 2.67$ g/cm^3; $x_r = 3.8$ cm), η_r could ordinarily be computed from equation 15 by substituting the peak Co^{60} counts obtained in the reference measurements for N_1 and N_2.

50. The family of reference curves obtained by measuring the Co^{60} radiation through various thicknesses equivalent to those of aluminum is shown in fig. 6. Instead of all occurring in the same channel for each measurement, the peak counts remained located near the same channel for thicknesses equivalent to aluminum between 57.8 and 76.2 cm, but shifted to higher numbered channels for thicknesses less than 57.8 cm. Because of the shift in channel locations of the Co^{60} peak counts, it was necessary to adjust the number of counts in the peaks for each measurement by the ratio of the channel location of the peak counts for each measurement to the average channel location of the peak for all measurements. Thus equation 15 must be written

$$L_2 N_2 = L_1 N_1 \, \exp\left(-\eta_r \rho_r x_r\right) \tag{16}$$

and

$$\eta_r = \frac{\ln\left(L_1 N_1 / L_2 N_2\right)}{\rho_r x_r} \tag{17}$$

where

L_1 = ratio of the channel location of the photon counts N_1 to the average channel location of the photon counts for all reference measurements

L_2 = ratio of the channel location of the photon counts N_2 to the average channel location of the photon counts for all reference measurements

51. The channel location of the Co^{60} peak counts in the reference measurements was determined in the following manner:

a. If the channel containing the greatest number of counts in a reference spectrum (fig. 6 and table 1) contained at least 1 percent more counts than either the next higher or next lower channel, the peak counts were considered located in

18
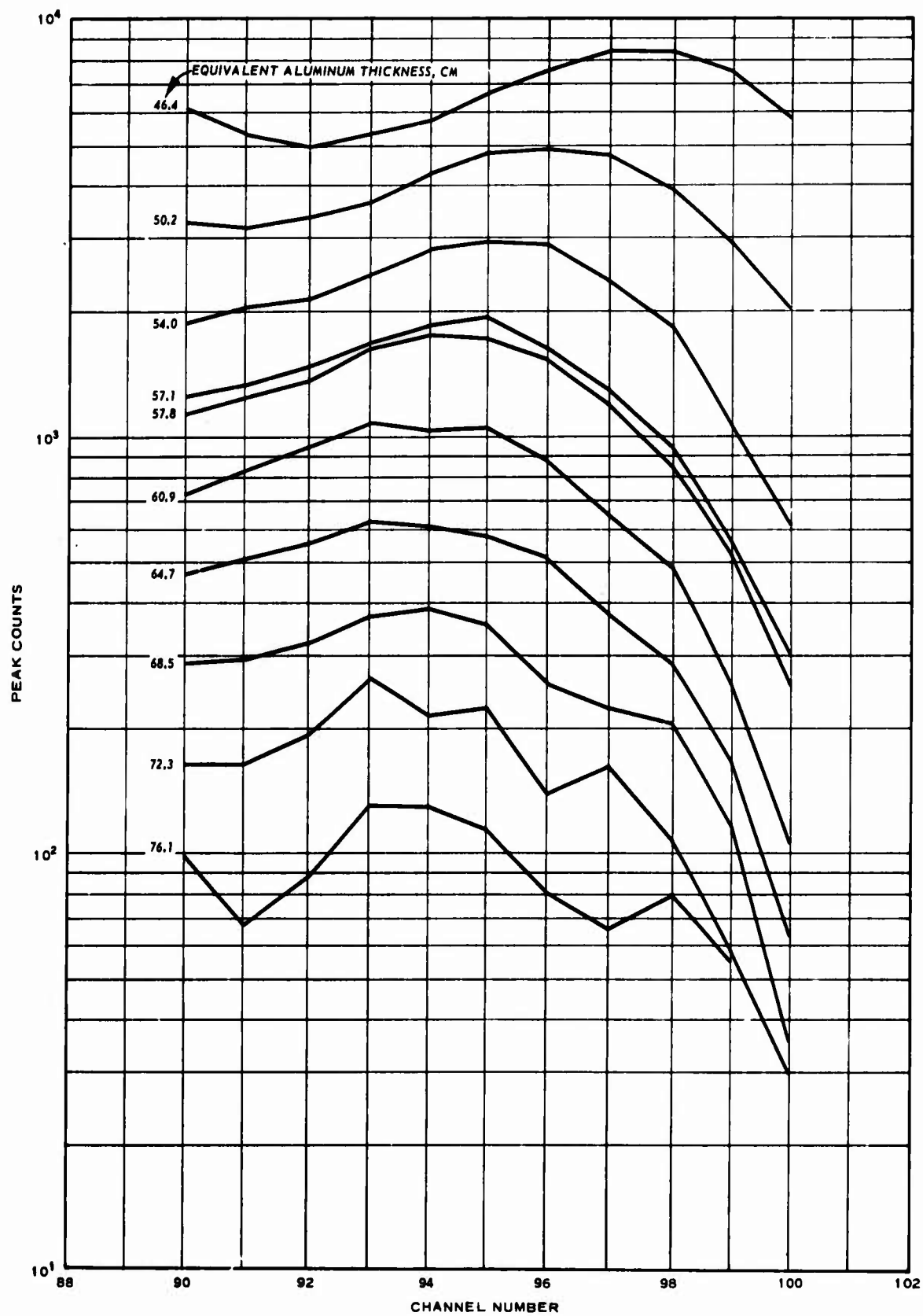
Fig. 6. Reference curves for equivalent aluminum
thickness and a cobalt 60 source

the channel containing the greatest number of counts.

 b. If the channel containing the greatest number of counts had fewer than 1 percent more counts than either the next higher or next lower channel, the peak counts were considered located midway between the channel containing the greatest number of counts and the channel containing less than 1 percent fewer counts.

 c. In the spectrum for an equivalent aluminum thickness of 60.9 cm, which contained peak counts in both channels 93 and 95, the peak was considered located in channel 94, since channels 93 and 95 contained nearly the same number of counts.

 d. The location of the peak counts was not determined for the spectra for an equivalent aluminum thickness of 72.3 or 76.1 cm. The fluctuations in counts from channel to channel in the spectrum for the former and the negative counts in the spectrum for the latter indicate that counts accumulated for these measurements with the Co^{60} source were not significantly greater than the background spectra for these measurements.

52. The locations of the peak Co^{60} counts determined in this manner for the eight reference spectra that were considered and the average channel location of the peak counts for all of these spectra are tabulated below.

Equivalent Aluminum Thickness, cm	Location of Cobalt 60 Peak Counts, Channel	L_i	N , Counts	η_r , cm^2/g
46.4	97.5	1.03	8356	0.05426
50.2	96.0	1.01	4914	0.05235
54.0	95.0	1.00	2918	0.05155
57.8	94.0	0.99	1747	
57.1	95.0	1.00	1911	0.06152
60.9	94.0	0.99	1034	0.05062
64.7	93.0	0.98	62.	0.04701
68.5	94.0	0.99	384	
	Avg 94.8			Avg 0.05289

53. The average location of the Co^{60} peak counts was channel 94.8. The value for L_i is the ratio of the Co^{60} peak location of each spectrum to 94.8. The number of counts N was taken directly from table 1 for each

spectrum except for N for an equivalent aluminum thickness of 46.4 cm, which is the average of counts in channels 97 and 98. The mass attenuation coefficient of the reference plates η_r was computed by equation 17 for each thickness of aluminum (not equivalent thickness). Then the average mass attenuation coefficient for all aluminum thicknesses, $0.0529 \text{ cm}^2/\text{g}$, was used in equation 14 to compute the sand density.

54. Evaluation of $\eta_{\alpha\ell}$. Since the aluminum plates and the aluminum tubes forming the source access holes were both measured with Co^{60}, $\eta_{\alpha\ell}$ in both cases was considered equal to $0.0529 \text{ cm}^2/\text{g}$.

55. Determination of η_s . The mass attenuation coefficient for sand and that for aluminum for an energy level of 1.25 Mev are available in published tables.[8] Therefore, the mass attenuation coefficient for sand at the energy level of Co^{60} (E = 1.33 Mev) could be determined by the equation

$$\frac{\eta_s(1.25)}{\eta_{\alpha\ell}(1.25)} = \frac{\eta_s(1.33)}{\eta_r(1.33)} \tag{18}$$

where

> $\eta_s(1.25)$ = mass attenuation coefficient of sand when E = 1.25 Mev, equals $0.0567 \text{ cm}^2/\text{g}$ (from reference 8)
>
> $\eta_{\alpha\ell}(1.25)$ = mass attenuation coefficient of aluminum when E = 1.25 Mev, equals $0.0548 \text{ cm}^2/\text{g}$ (from reference 8)
>
> $\eta_s(1.33)$ = mass attenuation coefficient of sand when E = 1.33 Mev, equals $0.0547 \text{ cm}^2/\text{g}$ (from equation 18)
>
> $\eta_r(1.33)$ = mass attenuation coefficient of aluminum plates when E = 1.33 Mev, equals $0.0529 \text{ cm}^2/\text{g}$ (from paragraph 53)

56. Determination of η_w . In the same manner, the mass attenuation coefficient of wood η_w was determined by the equation

$$\frac{\eta_w(1.25)}{\eta_{\alpha\ell}(1.25)} = \frac{\eta_w(1.33)}{\eta_r(1.33)} \tag{19}$$

where

> $\eta_w(1.25)$ = mass attenuation coefficient of wood when E = 1.25 Mev, equals $0.0607 \text{ cm}^2/\text{g}$ (from reference 8)

21

$\eta_W(1.33)$ = mass attenuation coefficient of wood when $E = 1.33$ Mev, equals 0.0586 cm^2/g (from equation 19)

57. Determination of ρ_r, $\rho_{\alpha\ell}$, and ρ_W. The purity of the aluminum used in the gamma-ray measurements was not known, so density values published in available tables could not be used. Therefore, the density of the aluminum plates ρ_r was determined from gravimetric measurements and found to be 2.67 g/cm^3. This value was also used as the density of the aluminum tubes $\rho_{\alpha\ell}$. The density of wood ρ_W was also determined by gravimetric measurement to be 0.50 g/cm^3.

58. Determination of $x_{\alpha\ell}$, x_W, x_r, and D_r. The thicknesses of the walls of the aluminum tubes $x_{\alpha\ell}$, of the wood x_W, and of the reference plates x_r were measured in a conventional manner. The distance D_r was measured at the time the reference measurements were made. Values for these parameters were as follows:

$$x_{\alpha\ell} = 0.483 \text{ cm}$$

$$x_W = 1.27 \text{ cm}$$

$$x_r = 64.7 \text{ cm}$$

$$D_r = 159.7 \text{ cm}$$

59. Evaluation of D_s and x_s. The center-to-center distance from source to detector for measurements on the soil D_s and the thickness of the soil x_s were measured at the time gamma radiation was measured.

60. Evaluation of K_i. To determine the value for K_i, it was necessary to multiply by 10 the counts in each channel of the reference spectrum to adjust for the difference in the live time for which the computer program was written (100 min) and the live time of the reference measurements (10 min), as explained in paragraph 45. A typical soil measurement (run No. 1732-1731) and the reference measurement ($\times$ 10) for an equivalent aluminum thickness of 64.7 cm are shown in fig. 7. This particular reference spectrum was selected because the counts defining it were close to those measured through sand and the channels defining this spectrum always contained a greater number of counts than the corresponding channels defining the soil spectra. The number of counts in each channel and the average

Fig. 7. Comparison of peak counts for soil measurement and reference measurement, run No. 1732-1731
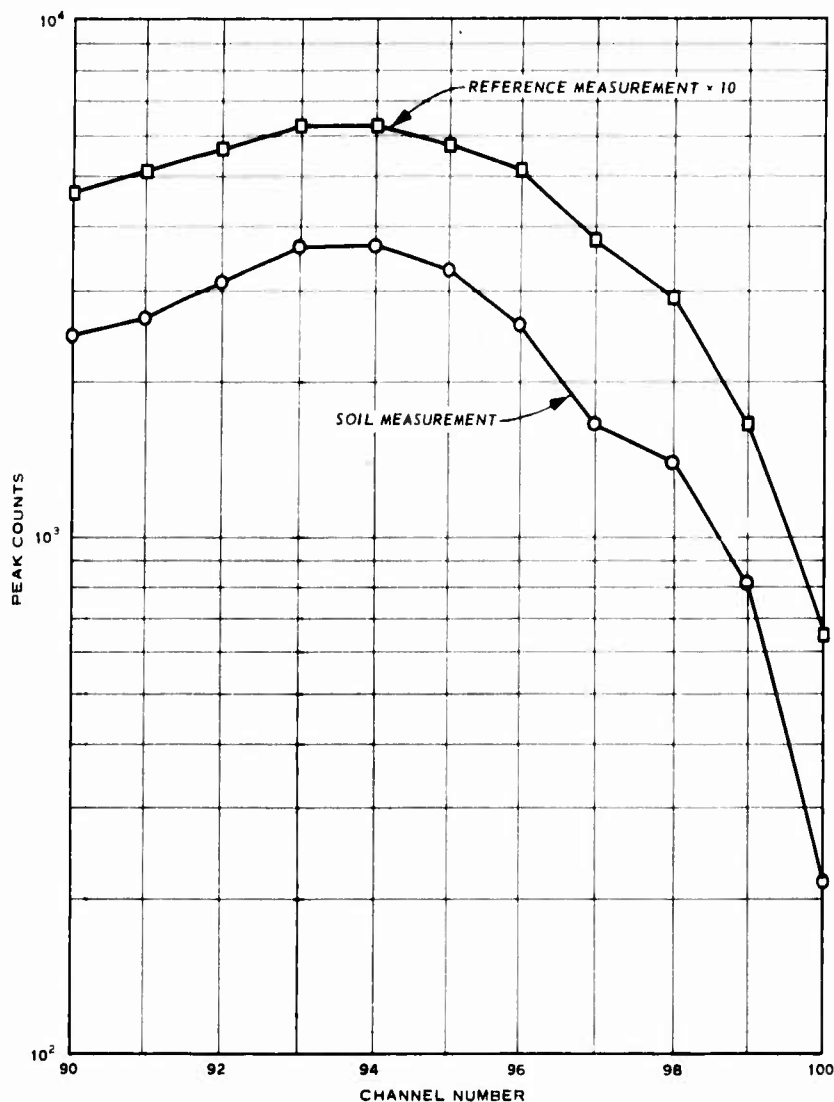
counts of the two spectra are tabulated below.

Channel No.	Reference Measurements (x 10)	Soil Measurement	Channel No.	Reference Measurements (x 10)	Soil Measurement
90	4680	2476	96	5160	2570
91	5120	2629	97	3780	1642
92	5580	3098	98	2880	1398
93	6250	3618	99	1660	816
94	6130	3642	100	640	213
95	5770	3286	Avg	4331.8	2308.0

61. The value of K_i , the average proportional change in the vertical direction required to achieve coincidence or near coincidence of the soil and reference spectrum, was determined by the equation

$$K_i = \frac{N_s(\text{avg})}{N_r(\text{avg})} \tag{20}$$

where

$N_s(\text{avg})$ = the average of the number of photon counts contained within channels 90-100 detected in a 10-min live time for soil measurements

$N_r(\text{avg})$ = the average of the number of photon counts contained within channels 90-100 detected in a 10-min live time for the reference measurement

For run No. 1732-1731

$$K_i = \frac{N_s(\text{avg})}{N_r(\text{avg})} = \frac{2308.0}{4331.8} = 0.53 \tag{21}$$

62. In practice, the value of K_i was determined by overlaying the reference spectrum on each of the soil spectra and, while maintaining horizontal alignment of the two spectra, adjusting the reference spectrum in the vertical direction until it was in coincidence or near coincidence with the soil spectrum. With the two spectra aligned in this manner, K_i was found by dividing a convenient number on the vertical axis of the soil spectrum by the number on the reference spectrum directly underlying it.

63. Evaluation of L_i . The average proportional change in the horizontal direction L_i required to achieve coincidence or near coincidence of the soil and reference spectra was found by the equation

$$L_i = \frac{C_s}{C_r} \tag{22}$$

where

C_s = channel location of Co^{60} photopeak in the soil spectrum

C_r = channel location of Co^{60} photopeak in the reference spectrum, equals 93.0 for the reference spectrum used in this study

The criteria stated in paragraph 51 were used to determine the location of the peak Co^{60} counts in the reference spectrum and in the soil measurements. By using run No. 1732-1731 for an example, the peak counts were determined to be located in channel 93.5. Therefore,

24

$$L_i = \frac{C_s}{C_r} = \frac{93.5}{93.0} = 1.01 \tag{23}$$

64. Summary. Constants used to compute the density for all measurements and values determined for run No. 1732-1731 are summarized below.

    a. Photon count:

Channel No.	Source in Position (Run No. 1732)	Source Removed (Run No. 1731)
90	9,597	7,121
91	9,165	6,536
92	9,406	6,308
93	9,623	6,005
94	9,766	6,124
95	10,126	6,840
96	10,421	7,851
97	10,852	9,210
98	12,463	11,065
99	15,426	14,610
100	20,053	19,840
Total	126,898	Total 101,510

    b. Constants:

$\eta_r = 0.0529 \ cm^2/g$ $\qquad$ $\rho_{\alpha\ell} = 2.67 \ g/cm^3$

$\eta_w = 0.0586 \ cm^2/g$ $\qquad$ $D_r = 159.7 \ cm$

$\eta_{\alpha\ell} = 0.0529 \ cm^2/g$ $\qquad$ $x_r = 64.7 \ cm$

$\eta_s = 0.0547 \ cm^2/g$ $\qquad$ $x_w = 1.27 \ cm$

$\rho_r = 2.67 \ g/cm^3$ $\qquad$ $x_{\alpha\ell} = 0.48 \ cm$

$\rho_w = 0.50 \ g/cm^3$ $\qquad$ $C_r = 93.0$

    c. Variables:

$D_s = 141.6 \ cm$ $\qquad$ $K_i = 0.53$ $\qquad$ $L_i = 1.01$

$x_s = 120.8 \ cm$ $\qquad$ $C_s = 93.5$

    d. Result of Computation:

$\rho_s = 1.50 \ g/cm^3$

Test Results

65. Data from the gamma-ray tests are summarized in table 2 and listed in detail in table 3. The access hole numbers identify the detector locations during the measurements and correspond to the numbers in fig. 5. Soil sample heights were measured from the bottom of the pit to the top surface of the soil. The source and detector heights were measured from the bottom of the source and the detector to the bottom of the pit.

66. The density measurements listed in tables 2 and 3 are presented graphically in plates 1 and 2 as profiles of density versus source height for the various access holes. A comparison of densities at various source heights is graphically presented in plates 3 and 4. Plate 5 shows measurements made on sample 1 when it had been constructed to a height of approximately 51.0 cm compared with measurements made after the sample had been constructed to its final height of approximately 121.8 cm.

Top layer measurements

67. Measurements made near the surface of the sample were inaccurate because radiation from the source "leaked" over the top of the soil to the detector. This leakage resulted in a combination of soil and air above the soil affecting the measurement. Since the density of air is less than the density of the soil, an increase in counting rate occurred that resulted in an increase in the dead time to approximately 15 percent. A dead time of 15 percent was considered maximum for these measurements.

68. The errors resulting from measurements made near the surface of the sample are evident in plate 4. The final measurements on sample 2 were made approximately 3.76 cm beneath the surface of the sample (source height 120.7 cm). The densities measured at this depth were nonuniform and varied from 1.36 to 1.61 g/cm^3. Measurements at all other depths were between 1.45 and 1.56 g/cm^3.

Comparison of densities measured during and after sample construction

69. Gamma radiation was measured at three heights during construction of sample 1 and again at the same heights after completion of construction. The initial measurements were made on the three layers closest to the

bottom of the sample after it had been constructed to a height of approximately 51.0 cm. Final measurements were made after a sample height of 121.8 cm had been reached. These measurements are compared in plate 5. The density can be seen to have increased slightly in all holes after the initial measurements were made. This increase probably was caused by an increase in static pressure in the lower level of the pit as the sample was constructed.

Analysis of Data

70. From the measurements in this study, an estimate can be made of the minimum and maximum allowable thicknesses of the sample, the optimum thickness of the sample consistent with the accuracy desired, the suitability of the Co^{60} source for these measurements, the thickness of the layer that affects the density measurement, and the accuracy and suitability of nuclear density measurements relative to nonnuclear measurements.

Sample thickness

71. **Minimum.** The minimum sample thickness is controlled by the photon flux that can impinge upon the detector without adversely affecting either its gain or stability. The maximum flux for the detector used in this study is approximately 10,000 counts/sec.[9]

72. To determine the minimum sample thickness, values for a typical measurement (run No. 1732-1731, paragraph 64) were substituted in equation 5. (Note: In this and subsequent determinations, the number of counts in each channel of the computer output was divided by 10 so that the actual counts from the source and background are considered.)

    <u>a</u>. Let N_s equal the sum of counts stored in channels 001 through 199 divided by the live time (600 sec). $N_s = 93$ counts/sec. All channels must be considered since the detector responds to radiation from all sources.

    <u>b</u>. Substitute in equation 5 to obtain

$$93 = N_o \left(\frac{D_o}{141.6} \right)^2 \exp{-(0.0547)(1.5)(120.8)} \qquad (24)$$

c. Assume a constant ΔD , where $\Delta D = D_s - x_s$.

d. Substitute values from paragraph 64, $\Delta D = 141.6$
- 120.8 = 20.8 .

e. Let $D_s = x_s + 20.8$ and $N_s = 10,000$ (paragraph 71), and obtain values for η_s and ρ_s from paragraph 64.

f. Substitute these values in equation 5 to obtain:

$$10,000 = N_o \left(\frac{D_o}{x_s + 20.8} \right)^2 \quad \exp -(0.0547)(1.5)(x_s) \quad (25)$$

g. Solve equation 24 for $N_o D_o{}^2$ and substitute this value in equation 25. Then by iteration, a value for x_s can be found that will solve equation 25. Solving for x_s in this manner yields 73.7 cm, the minimum sample thickness.

73. Maximum. The number of counts that will be detected from a radioactive source within a given live time will decrease as the sample thickness increases. On the other hand, an increase in sample thickness will have no effect on the number of counts detected from the background. Therefore, at some sample thickness, the counts from the source will equal the counts from the background. At any greater thickness, background counts will exceed counts from the source.

74. If the soil sample, in this case sample 2, is assumed to have the same density and moisture content throughout and the background radiation remains at a constant level, the maximum thickness of the sample for density measurements in this soil material can be determined. Substitute values from run No. 1732-1731 in equation 5 in the following manner:

a. Let $D_s = \Delta D + x = 20.8 + x$

b. Let $N_s = N_{s+b} - N_b$
where

       N_{s+b} = total number of counts in channels 90 through 100 for measurement with the Co^{60} source in position, equals 12,690

       N_b = total number of counts in channels 90 through 100 for measurement with the radioactive source removed, equals 10,151

<u>c</u>. From run No. 1732-1731, obtain values for η_s , ρ_s , and x_s (paragraph 64).

<u>d</u>. Substitute these values in equation 5 and solve for $N_o D_o^2$.

<u>e</u>. Substitute this value for $N_o D_o^2$ in equation 5 and replace the value for x from run No. 1732-1731 (120.8 cm) with other values to determine what N_s would have been if the sample thickness had been some thickness x . In table 4 predicted values for N_s are shown for various sample thicknesses x_s between 100.00 and 151.25 cm.

75. Statistically, the number of counts detected within a certain live time obeys the Poisson distribution.[7,10] Therefore, the standard deviation σ of the number of counts N is

$$\sigma = \sqrt{N} \qquad (26)$$

Statistical uncertainty exists for both soil and background measurements, i.e. measurements made with and without the radioactive source in position, so that both N_{s+b} and N_b must be considered. Therefore,[11]

$$\sigma_N = \sqrt{N_{s+b} + N_b} \qquad (27)$$

Since N_b will remain constant independent of a changing x_s , and at the same time N_{s+b} decreases with increasing values of x_s , σ_N will decrease as x_s increases. Table 4 shows values for σ_N for various values of x_s .

76. The maximum thickness is reached when the number of counts N_s equals the standard deviation σ_N . Therefore, from table 4, the maximum thickness is found to be approximately 151.12 cm.

77. <u>Optimum.</u> As the sample thickness x_s is increased, the error in density measurements can be expected to increase. By using the various values for x_s , N_s , and σ_N listed in table 4, the error can be predicted. In equation 5:

<u>a</u>. Again let $D_s = 20.8 + x_s$.

    b. Substitute the value for $N_o D_o^2$ previously computed (paragraph 74d).

    c. Let η_s = 0.0547 (from run No. 1732-1731).

    d. Substitute the various values for x_s, N_s, and σ_N in equation 5 and solve for predicted density ρ_p.

    e. Determine the error in percent density by the equation

$$\rho_{p(\%)} = \left[(1.5 - \rho)/1.5\right] 100 \qquad (28)$$

    (This statement assumes the actual density of the sample to be 1.5 g/cm^3.)

The results of computations of ρ_p and $\rho_{p(\%)}$ for various sample thicknesses x_s are listed in table 4.

    78. Optimum thickness is achieved when the sample thickness is small enough to permit source counts to exceed the standard deviation, yet not small enough to damage the detector crystal. For any particular test situation, a maximum thickness must be chosen that is consistent with the accuracy required. For the measurements discussed herein, the predicted error in density was approximately 0.53 percent.

Radiation source suitability

    79. Penetration. The mass attenuation coefficient η_s of sand was found to be 0.0547 cm^2/g when Co^{60} with an energy level of 1.33 Mev was used as the source of radiation. If a source with a lower energy level had been used, the mass attenuation coefficient would have been greater. For example, if cesium 137 with an energy level of 0.662 Mev had been selected as the radiation source, the mass attenuation coefficient of sand[8] would have been approximately 0.0778 cm^2/g. For the same live time, the number of counts N that will be detected from a source through sand with a density ρ and thickness x will be less for Cs^{137} than for Co^{60} (see equation 1). As a result, the maximum allowable sample thickness would be decreased from that determined with Co^{60} as the source.

    80. Background radiation. A typical spectrum of gamma radiation from Yuma sand is shown in fig. 8, where the natural radioactivity of the soil measured in a 40-min live time is presented. Even though the counts
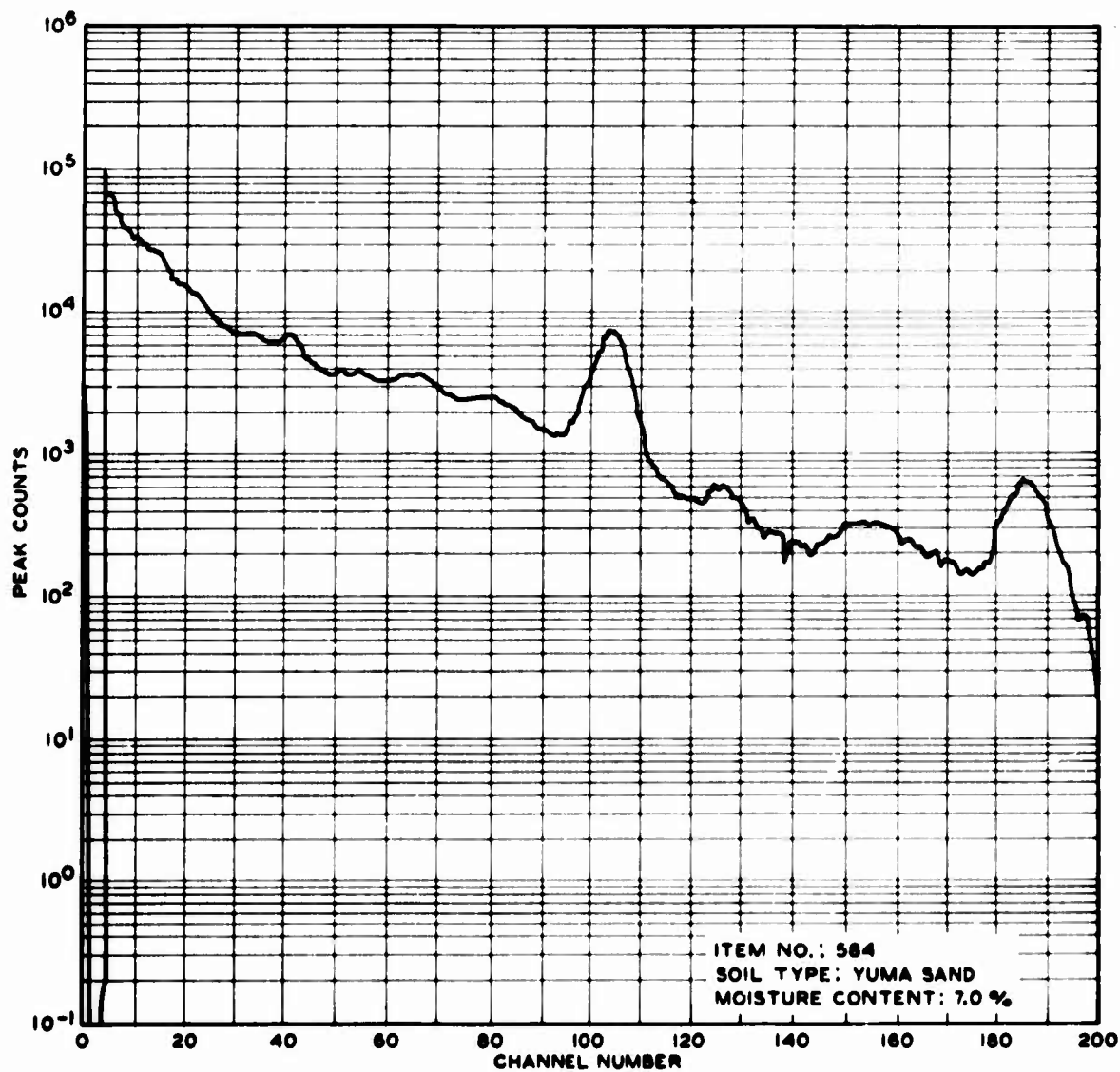
Fig. 8. Typical spectrum of gamma radiation
from Yuma sand (from reference 7)

per channel are greater than those for a 10-min live time, the shape of the
spectrum is characteristic of background measurements made for density deter-
minations. Except for photopeaks due to the naturally occurring radioac-
tive constituents in the soil, background radiation generally decreases as
energy level (channel number) increases, so that measurements with a source
of radiation having a higher energy level, such as Co^{60} ($E = 1.33$ Mev),
result in lower statistical error in the number of counts than measure-
ments with a lower energy source, such as Cs^{137} ($E = 0.662$ Mev).

31

Layer thickness affecting measurement

81. If a gamma-ray photon emitted from a source has an initial energy E between 1 and 2 Mev and passes through a material placed between the source and a detector (S and D, respectively, fig. 9) without colliding with an electron whose binding energy is small compared to that of the gamma ray, E will be detected. However, if a collision should occur in the material, the photon will give up some of its energy to the electron and proceed with reduced energy (E') along an altered path (CD in fig. 9) to the detector. The energy E' at D depends upon the initial photon energy E and the scattering angle θ as shown by the equation[8]

$$E' = \frac{E}{1 + (1 - \cos\theta)(E/0.5110)} \tag{29}$$

For small scattering angles, E' ≈ E . But as θ increases, E' diminishes. The energy of photons having a high initial energy, such as those of Co^{60}, diminishes more rapidly as the scattering angle increases than does the energy of photons having lower initial energy, such as those of Cs^{137}, as shown in fig. 10.

82. The scattering angle θ is formed at the intersection of the lines extending to the location of the scattering event C from the source S and from the detector D. In a plane, the locus of all points C (fig. 11) at which two lines intersect at a given angle θ and extend to points S and D , respectively, is an arc of a circle terminated at points S and D. Rotating the arc around the line $\overline{SD}$ defines the boundary of the material that affects measurements. It follows then that if the length of $\overline{SD}$ and the scattering angles θ along the various paths $\overline{SCD}$ are known, the boundaries of the volume of soil or the thickness of the layer of soil R affecting measurements can be determined.

83. The length $\overline{SD}$ can be measured, but the method for determining the scattering angle is less direct. If a spectrum of the number of gamma-ray counts versus energy level (channel number) is measured, discrimination between unscattered photons and photons scattered through small angles can be accomplished by selecting for analysis the number of counts within a certain energy range (group of channels) around the peak energy of

32

Fig. 9. Gamma-ray photons
passing through a material in
which scattering occurs

CURVES CALCULATED FROM

$$E' = \frac{E}{1 + (1 - \cos\theta)(E/0.5110)}$$

COBALT 60
(E = 1.333 MEV)

CESIUM 137
(E = 0.662 MEV)

SCATTERING ANGLE θ, DEG

ENERGY OF SCATTERED PHOTON E', MEV
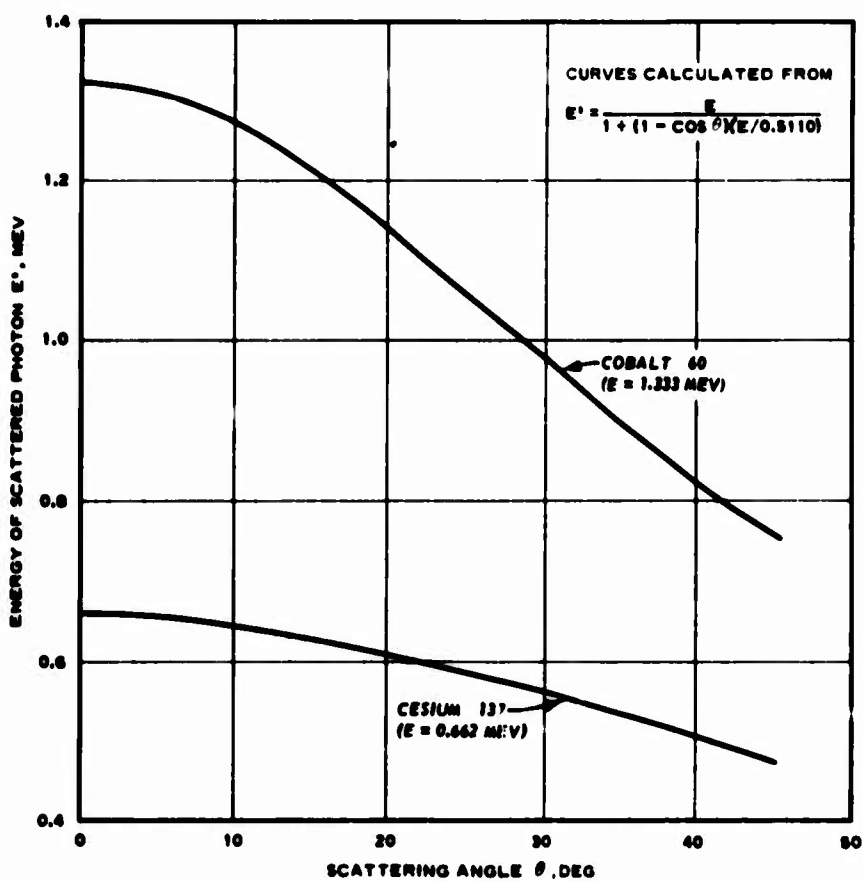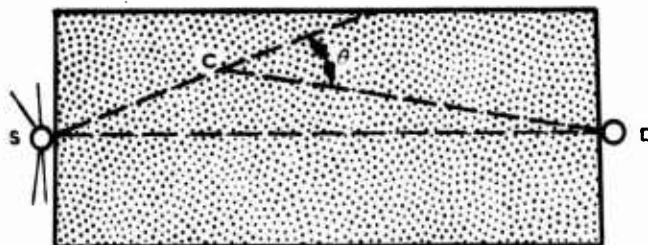
Fig. 10. Effects
of scattering angle
on scattered photon
energy for Co[60] and
Cs[137]

Fig. 11. Volume of material
affecting measurement

33
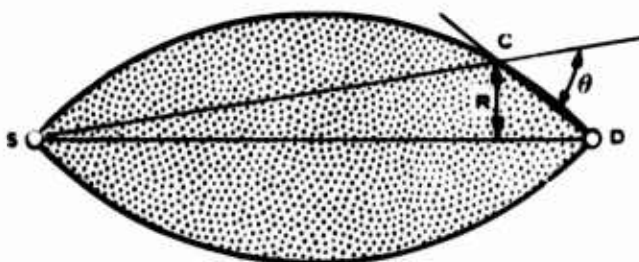
unscattered photons. Equation 29 restated to give a solution for the scattering angle θ is

$$\theta = \cos^{-1}\left[1 - \frac{0.5110(E - E')}{EE'}\right] \tag{30}$$

By establishing a lower limit for E', only photons scattered in an angle of θ or less will be considered. This restricts the boundaries of the volume of soil affecting the measurement being taken; and the thickness of the layer R that affects the measurement can therefore be determined by the following equation:

$$R = \overline{SD} \tan\left(\frac{\theta}{2}\right) \tag{31}$$

84. For density determinations, gamma-ray counts located in channels 90 through 100 were considered. The lower limit for E' was therefore 90×0.014168 Mev $= 1.27512$ Mev, and $\theta = 10.6°$. From equation 31, the thickness of the layer R affecting the measurements in this study was 14.0 cm. Actually, the thickness is slightly greater, since equation 31 is applicable only for a point source and detector.

Comparison of nuclear and nonnuclear density measurements

85. The density of soil at a number of locations adjacent to the detector access holes was determined by conventional nonnuclear methods. The values obtained in this manner are compared in the following tabulation with density values determined by nuclear techniques:

Sample No.	Height in Sample cm	Access Hole No.	Nonnuclear Density g/cm^3	Nuclear Density g/cm^3	Difference g/cm^3 (Nonnuclear - Nuclear)
1	50.8	1	1.44	1.42	0.02
		4	1.43	1.41	0.02
2	38.1	1	1.51	1.47	0.04
		4	1.50	1.49	0.01

(Continued)

34

Sample No.	Height in Sample cm	Access Hole No.	Nonnuclear Density g/cm^3	Nuclear Density g/cm^3	Difference g/cm^3 (Nonnuclear-Nuclear)
2	63.5	1	1.55	1.52	0.03
		2	1.56	1.52	0.04
		3	1.56	1.54	0.02
		4	1.56	1.53	0.03
		5	1.56	1.53	0.03
		6	1.55	1.49	0.06
	88.9	1	1.54	1.47	0.07
		4	1.54	1.45	0.09

86. There is good agreement between the nuclear and nonnuclear densities, suggesting that the two techniques might be complementary in engineering applications requiring both surface and subsurface density measurements in a section of soil. Whereas it is difficult to obtain subsurface density measurements with conventional techniques, gamma-ray measurements are feasible if access holes can be provided. It is important to remember, however, that conventional measurements normally provide the density at the spot where the sample is taken, while nuclear techniques measure the average density of a volume of soil between the source and detector.

PART V: CONCLUSIONS AND RECOMMENDATIONS

Conclusions

87. Based on the measurements and subsequent density determinations reported herein, the following conclusions are drawn:

    a. Gamma-ray measurements can be used as an effective means of measuring sand density provided the thickness of the sample is such that background radiation and detector instability do not affect the measurement accuracy.

    b. Measurements made close to the surface of the sample have limited value unless shielding is used to reduce the radiation "leakage" over the top of the sample to the detector.

Recommendations

88. It is recommended that:

    a. This method be used more extensively for nondestructive soil density measurements.

    b. No more feasibility studies be made, since the basis of this method is a simple physical phenomenon and is sufficiently understood.

LITERATURE CITED

1. Belcher, D. J., Cuykendall, T. R., and Sack, H. S., "The Measurement of Soil Moisture and Density by Neutron and Gamma-Ray Scattering," Technical Development Report No. 127, 1950, Civil Aeronautics Administration, Washington, D. C.

2. Rush, E. S. and Reinhart, K. G., "Field Tests of Nuclear Instruments for the Measurement of Soil Moisture and Density," Miscellaneous Paper No. 4-117, Mar 1955, U. S. Army Engineer Waterways Experiment Station, CE, Vicksburg, Miss.

3. Belcher, D. J., Cuykendall, T. R., and Sack, H. S., "Nuclear Meters for Measuring Soil Density and Moisture in Thin Surface Layers," Technical Development Report No. 161, Feb 1952, Civil Aeronautics Administration, Technical Development and Evaluation Center, Indianapolis, Ind.

4. Carlton, P. F., et al., "Modifications and Tests of Radioactive Probes for Measuring Soil Moisture and Density," Technical Development Report No. 194, Mar 1953, Civil Aeronautics Administration, Technical Development and Evaluation Center, Indianapolis, Ind.

5. Beckett, W. R. and Schreiner, B. G., "Study of Nuclear Probes for Determination of Airfield Densities and Moistures," Miscellaneous Paper No. 4-199, Mar 1957, U. S. Army Engineer Waterways Experiment Station, CE, Vicksburg, Miss.

6. Hampton, E., "Report on the Use of Nuclear Moisture and Density Probes for Controlling Compaction on Airfield Pavement Construction," Jan 1960, U. S. Army Engineer District, Detroit.

7. Lundien, J. R., "Terrain Analysis by Electromagnetic Means; Laboratory Investigations in the 0- to 2.82-Mev Gamma-Ray Spectral Region," Technical Report No. 3-693, Report 3, Nov 1967, U. S. Army Engineer Waterways Experiment Station, CE, Vicksburg, Miss.

8. Blizard, E. P., 7.3 Nuclear Radiation Shielding, McGraw-Hill, New York, 1958.

9. Harshaw Chemical Company, Guaranteed Stability Specifications for Integral Line and Matched Window Line Scintillation Detectors, Cleveland, Ohio.

10. Friedlander, G., Kennedy, J. W., and Miller, J. M., Nuclear and Radiochemistry, 2d ed., Wiley, New York, 1964.

11. Guttman, I. and Wilks, S. S., Introductory Engineering Statistics, Wiley, New York, 1965.

Table 1

<u>Photon Counts Per Channel for Reference Curves</u>

Equiv- alent Aluminum Thickness cm	Photon Counts for Indicated Channel Number										
	90	91	92	93	94	95	96	97	98	99	100
46.4	6138	5333	4981	5356	5788	6639	7482	8393	8319	7425	5815
50.2	3276	3168	3340	3661	4285	4783	4914	4746	3993	2966	2027
54.0	1877	2066	2120	2428	2819	2918	2880	2385	1826	1085	626
57.1	1252	1321	1481	1691	1848	1911	1631	1298	938	563	302
57.8	1140	1260	1377	1628	1747	1705	1531	1193	852	522	251
60.9	730	828	939	1083	1034	1066	884	649	492	256	108
64.7	468	512	558	625	613	577	516	378	288	166	64
68.5	288	293	320	371	384	354	257	226	207	118	36
72.3	163	163	193	266	217	226	140	161	108	59	30
76.1	98	67	88	130	130	115	81	66	80	56	-15

Table 2

<u>Summary of Results of Nuclear Density Measurements</u>

Sample No.	Soil Sample Height cm	Source Height cm	Density in g/cm^3 for Indicated Access Hole No.					
			1	2	3	4	5	6
1	51.0	12.7	1.41	1.42	1.41	1.43	1.42	1.43
		25.4	1.40	1.42	1.42	1.43	1.42	1.42
		38.1	1.43	1.43	1.43	1.44	1.44	1.44
	121.8*	12.7	1.41	1.42	1.43	1.43	1.42	1.45
		25.4	1.42	1.43	1.43	1.44	1.43	1.45
		38.1	1.43	1.44	1.45	1.46	1.45	1.46
		50.8	1.42	1.43	1.42	1.41	1.40	1.44
		63.5	1.43	1.44	1.42	1.43	1.41	1.43
2	124.5	12.7	1.45	1.47	1.48	1.47	1.48	1.46
		25.4	1.50	1.48	1.49	1.47	1.48	1.50
		38.1	1.47	1.49	1.50	1.49	1.48	1.47
		50.8	1.51	1.51	1.51	1.51	1.51	1.48
		63.5	1.52	1.52	1.54	1.53	1.53	1.49
		76.2	1.53	1.49	1.53	1.53	1.48	1.49
		88.9	1.47	1.48	1.49	1.45	1.46	1.48
		101.6	1.47	1.49	1.48	1.48	1.50	1.47
		114.3	1.50	1.53	1.52	1.51	1.56	1.56
		120.7*	1.55	1.52	1.61	1.36	1.58	1.44

* 121.9 cm for holes 1 and 6.

Table 3

Results of Nuclear Density Measurements

Sample 1 / Sample 2

Item No.	Access Hole No.	Soil Run No.	Background Run No.	Soil Sample Height* cm	Detector Height* cm	Source Height* cm	Soil Thickness x_s, cm	Distance Source to Detector D_s, cm	Vertical Channel Change K_1	Channel Location C_s	Soil Density ρ_s g/cm^3
											Sample 1
1	1	1534	1531	51.0	6.4	12.7	122.6	143.5	0.83	93.0	1.41
2	1	1537	1536		19.1	25.4	122.6	144.1	0.84	93.0	1.40
3	1	1541	1540		6.4	38.1	122.6	144.1	0.70	93.0	1.43
4	2	1546	1543		6.4	12.7	122.1	143.8	0.79	93.5	1.42
5	2	1550	1547		19.1	25.4	122.1	144.1	0.78	93.0	1.42
6	2	1554	1551		31.8	38.1	122.1	143.8	0.70	96.0	1.43
7	3	1558	1555		6.4	12.7	123.2	143.5	0.79	94.0	1.41
8	3	1562	1559		19.1	25.4	123.2	144.5	0.71	93.5	1.42
9	3	1566	1563		31.8	38.1	123.2	144.5	0.66	93.3	1.43
10	4	1557	1556		6.4	12.7	121.6	141.0	0.78	93.3	1.43
11	4	1561	1560		19.1	25.4	121.6	141.9	0.76	94.0	1.43
12	4	1565	1564		31.8	38.1	121.6	141.6	0.72	93.7	1.44
13	5	1545	1544		6.4	12.7	121.9	141.9	0.80	93.0	1.42
14	5	1549	1548		19.1	25.4	121.9	143.5	0.81	93.3	1.42
15	5	1553	1552		31.8	38.1	121.9	141.9	0.71	93.3	1.44
16	6	1533	1532		6.4	12.7	121.8	141.0	0.80	93.7	1.43
17	6	1538	1535		19.1	25.4	121.8	141.6	0.82	93.3	1.42
18	6	1542	1539		31.8	38.1	121.8	141.6	0.72	93.3	1.44
19	1	1598	1595	121.8	6.4	12.7	124.2	145.7	0.70	92.7	1.41
20	1	1602	1599		19.1	25.4	123.8	145.3	0.65	93.7	1.42
21	1	1607	1603		31.8	38.1	123.4	145.6	0.66	93.0	1.44
22	1	1610	1607		44.5	50.8	122.9	145.1	0.71	93.7	1.42
23	2	1614	1611		57.2	63.5	122.4	144.4	0.72	93.0	1.43
24	2	1578	1575		6.4	12.7	122.7	144.8	0.74	91.7	1.41
25	2	1602	1599		19.1	25.4	123.8	145.2	0.65	93.7	1.42
26	2	1586	1583		31.8	38.1	122.0	144.8	0.68	93.0	1.45
27	2	1590	1587		44.5	50.8	121.7	145.2	0.76	93.7	1.42
28	2	1594	1591		57.2	63.5	121.3	143.4	0.73	94.0	1.42
29	3	1618	1615		6.4	12.7	122.9	144.2	0.70	93.5	1.43
30	3	1622	1619		19.1	25.4	123.0	144.6	0.67	93.3	1.43
31	3	1626	1623		31.8	38.1	123.1	145.0	0.60	92.7	1.45
32	3	1630	1627		44.5	50.8	123.2	144.4	0.74	92.7	1.42
33	3	1631	1631		57.2	63.5	122.3	143.4	0.73	94.0	1.41
34	4	1617	1616		6.4	12.7	121.1	142.0	0.80	93.5	1.44
35	4	1621	1620		19.1	25.4	121.0	141.9	0.77	93.3	1.43
36	4	1625	1624		31.8	38.1	120.9	141.8	0.48	93.5	1.46
37	4	1629	1628		44.5	50.8	120.9	141.8	0.96	93.3	1.41
38	5	1633	1632		57.2	63.5	120.8	141.7	0.83	93.0	1.43
39	5	1577	1576		6.4	12.7	121.3	139.8	0.87	93.0	1.42
40	5	1581	1580		19.1	25.4	121.6	148.1	0.72	93.3	1.43
41	5	1585	1584		31.8	38.1	121.8	142.8	0.66	93.0	1.45
42	5	1589	1588		44.5	50.8	122.0	141.4	0.93	93.5	1.40
43	6	1593	1592		57.2	63.5	122.3	141.7	0.83	93.3	1.41
44	6	1596	1597		6.4	12.7	120.3	141.2	0.76	93.3	1.45
45	6	1601	1600		19.1	25.4	120.4	141.3	0.76	93.7	1.45
46	6	1605	1604		31.8	38.1	120.5	140.5	0.73	93.3	1.46
47	6	1609	1608		44.5	50.8	120.7	140.7	0.81	93.5	1.44
48	6	1613	1612		57.2	63.5	120.8	141.1	0.82	93.5	1.43
											Sample 2
49	1	1665	1662	124.5	6.4	12.7	121.9	142.9	0.64	93.5	1.46
50	1	1669	1666		19.1	25.4	121.8	143.8	0.48	93.0	1.50
51	1	1673	1670		31.8	38.1	121.8	144.1	0.50	92.0	1.47
52	1	1677	1674		44.5	50.8	121.6	143.8	0.46	93.5	1.56
53	1	1681	1678		57.2	63.5	121.3	143.5	0.45	92.3	1.52

Sample 2 (continued)

Item No.	Access Hole No.	Soil Run No.	Background Run No.	Soil Sample Height* cm	Detector Height* cm	Source Height* cm	Soil Thickness x_s, cm	Distance Source to Detector D_s, cm	Vertical Change K_1	Channel Location C_s	Soil Density ρ_s g/cm^3
54	1	1685	1682	124.5	69.9	76.2	121.0	144.1	0.41	93.3	1.53
55	1	1689	1686		82.6	88.9	122.1	144.1	0.58	93.0	1.47
56	1	1693	1690		95.3	101.6	120.8	144.1	0.62	93.3	1.47
57	1	1695	1694		108.0	114.3	122.6	144.1	0.48	93.0	1.50
58	1	1699	1697		115.6	121.9	122.6	144.1	0.32	94.0	1.55
59	2	1705	1702		6.4	12.7	121.9	144.1	0.56	93.0	1.47
60	2	1709	1706		19.1	25.4	122.0	144.1	0.52	93.5	1.48
61	2	1713	1710		31.8	38.1	122.1	144.1	0.48	93.5	1.49
62	2	1717	1714		44.5	50.8	122.1	144.1	0.43	92.7	1.51
63	2	1721	1718		57.2	63.5	122.1	144.1	0.41	93.0	1.52
64	2	1725	1722		69.9	76.2	121.9	144.1	0.49	93.0	1.49
65	2	1729	1726		82.6	88.9	121.9	144.1	0.53	93.5	1.8
66	2	1733	1730		95.3	101.6	121.6	144.1	0.52	90.0	1.49
67	2	1737	1734		108.0	114.3	121.6	144.1	0.40	91.0	1.53
68	2	1736	1735		114.4	120.4	121.3	144.1	0.44	93.0	1.52
69	3	1745	1742		6.4	12.7	121.9	144.1	0.53	93.5	1.48
70	3	1749	1746		19.1	25.4	121.9	144.1	0.49	93.3	1.49
71	3	1753	1750		31.8	38.1	121.7	144.1	0.46	93.3	1.50
72	3	1757	1754		44.5	50.8	121.0	144.1	0.46	93.0	1.51
73	3	1761	1758		57.2	63.5	122.2	144.1	0.34	93.0	1.54
74	3	1765	1762		69.9	76.2	122.1	144.1	0.39	93.0	1.53
75	3	1769	1766		82.6	88.9	122.1	144.1	0.49	92.0	1.49
76	3	1773	1770		95.3	101.6	122.1	144.1	0.53	93.0	1.48
77	3	1777	1774		108.0	114.3	122.0	144.1	0.40	92.5	1.52
78	3	1776	1775		114.4	120.7	121.9	144.1	0.22	93.4	1.61
79	4	1744	1743		6.4	12.7	121.9	141.6	0.59	93.0	1.47
80	4	1748	1747		19.0	25.4	122.0	141.6	0.58	93.0	1.47
81	4	1752	1751		31.8	38.1	122.2	141.6	0.49	93.0	1.49
82	4	1756	1755		44.5	50.8	122.2	141.6	0.45	93.7	1.51
83	4	1760	1759		57.2	63.5	122.3	141.6	0.38	93.7	1.53
84	4	1764	1763		69.8	76.2	122.4	141.6	0.37	93.0	1.53
85	4	1768	1767		82.6	88.9	122.3	141.6	0.64	95.0	1.45
86	4	1772	1771		95.2	101.6	122.3	141.6	0.54	93.0	1.48
87	4	1781	1778		108.0	114.3	122.1	141.6	0.45	93.0	1.51
88	4	1780	1779		114.4	120.7	121.9	141.6	1.20	94.0	1.36
89	5	1704	1703		6.4	12.7	121.9	141.6	0.54	94.7	1.48
90	5	1708	1707		19.0	25.4	121.8	141.6	0.55	93.0	1.48
91	5	1712	1711		31.8	38.1	121.8	141.6	0.56	93.0	1.48
92	5	1716	1715		44.4	50.3	122.7	141.6	0.45	94.5	1.51
93	5	1720	1719		57.2	63.5	122.4	141.6	0.42	93.0	1.53
94	5	1724	1723		69.8	76.2	121.6	141.6	0.56	93.0	1.48
95	5	1728	1727		82.6	88.9	121.4	141.6	0.53	93.5	1.45
96	5	1732	1731		95.2	101.6	120.8	141.6	0.53	93.5	1.50
97	5	1741	1738		108.0	111.3	120.7	141.6	0.37	92.0	1.56
98	5	1740	1739		114.4	120.7	121.0	141.6	0.31	94.0	1.58
99	6	1664	1663		6.4	12.7	121.9	141.3	0.61	93.5	1.46
100	6	1668	1667		19.0	25.4	122.1	141.3	0.48	93.5	1.50
101	6	1672	1671		31.8	38.1	122.1	141.3	0.58	93.0	1.47
102	6	1676	1675		44.4	50.8	122.6	141.3	0.53	93.0	1.48
103	6	1680	1679		57.2	63.5	122.5	141.6	0.51	93.0	1.49
104	6	1684	1683		69.8	76.2	122.4	141.3	0.49	93.0	1.49
105	6	1688	1687		82.6	88.9	122.1	141.3	0.52	93.0	1.48
106	6	1692	1691		5.2	101.6	122.5	141.3	0.56	92.7	1.47
107	6	1699	1698		108.0	114.3	122.4	142.3	0.33	95.7	1.56
108	6	1700	1701		115.4	121.9	120.2	142.2	0.84	93.1	1.04

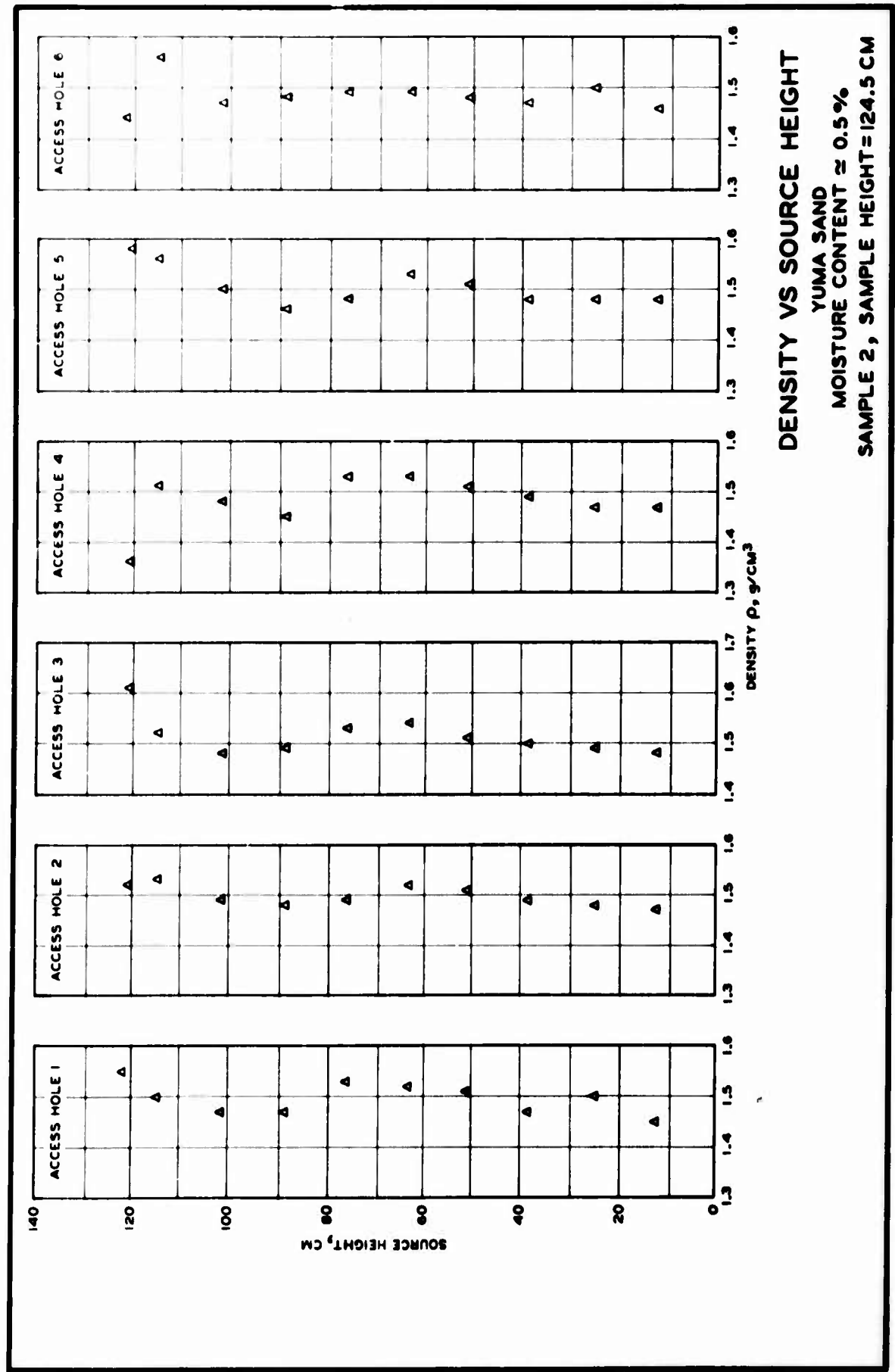* Heights are measured in cm from bottom of pit.

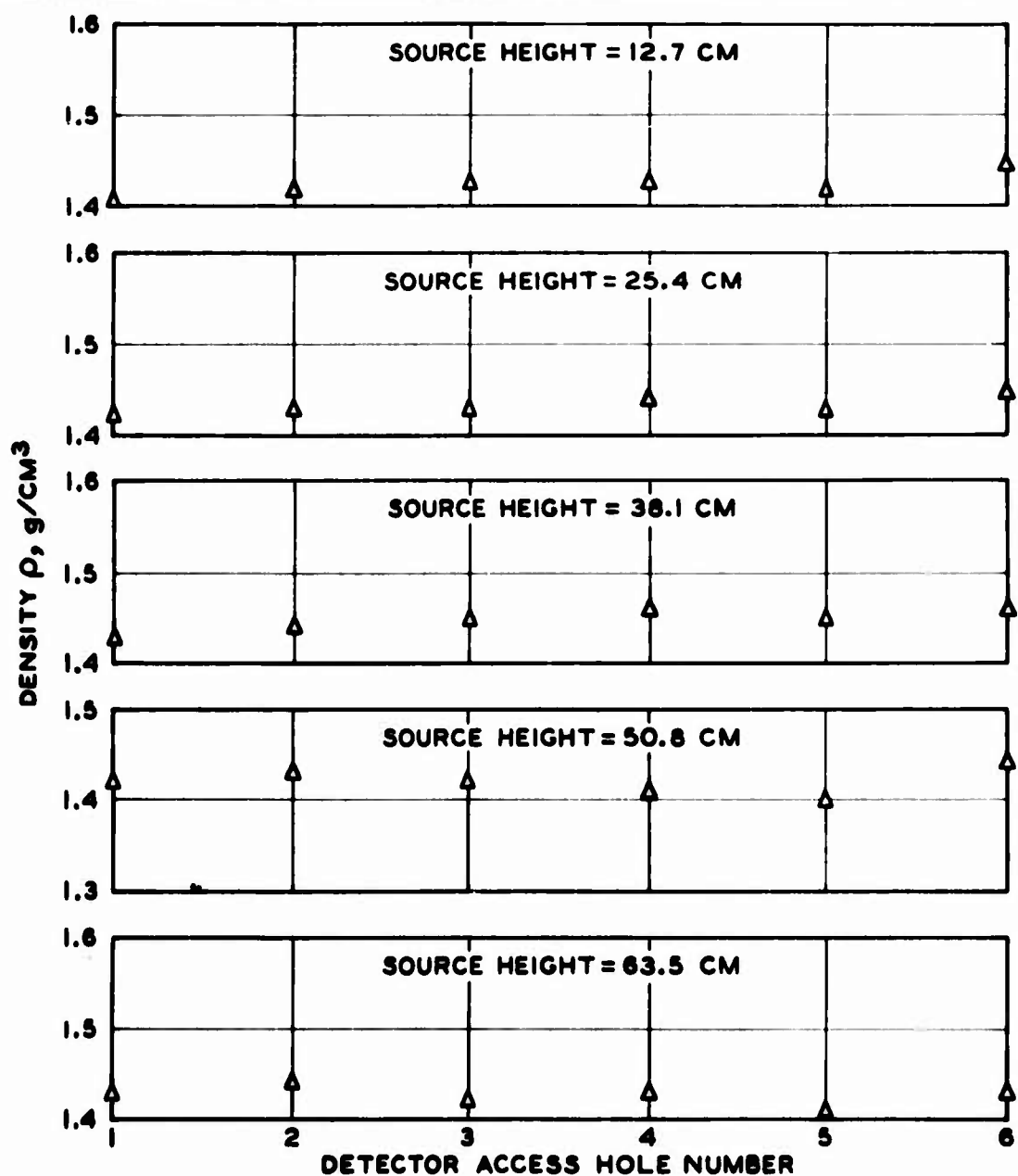Table 4

Effect of Sample Thickness on Measurement Accuracy

Soil Thickness x_s, cm	Source Photon Count, N_s	Source and Background Photon Count N_{s+b}	Standard Deviation σ_N	Predicted Density, ρ_p g/cm^3	% Error in Predicted Density $\rho_p (\%)$
100.00	19,224	29,375	198.8	1.498	0.13
105.00	11,761	21,911	179.1	1.497	0.20
110.00	7,281	17,369	165.9	1.495	0.33
115.00	4,443	14,593	157.3	1.494	0.40
120.00	2,742	12,893	151.8	1.492	0.53
125.00	1,697	11,847	148.3	1.487	0.87
130.00	1,052	11,203	146.1	1.482	1.20
135.00	654	10,805	144.7	1.473	1.80
140.00	407	10,558	143.9	1.461	2.60
145.00	254	10,405	143.4	1.444	3.73
150.00	159	10,310	143.0	1.422	5.20
150.25	155	10,306	143.0	1.421	5.27
150.50	152	10,303	143.0	1.419	5.40
150.75	148	10,299	143.0	1.418	5.47
151.00	145	10,296	143.0	1.417	5.53
151.25	141	10,292	143.0	1.416	5.60
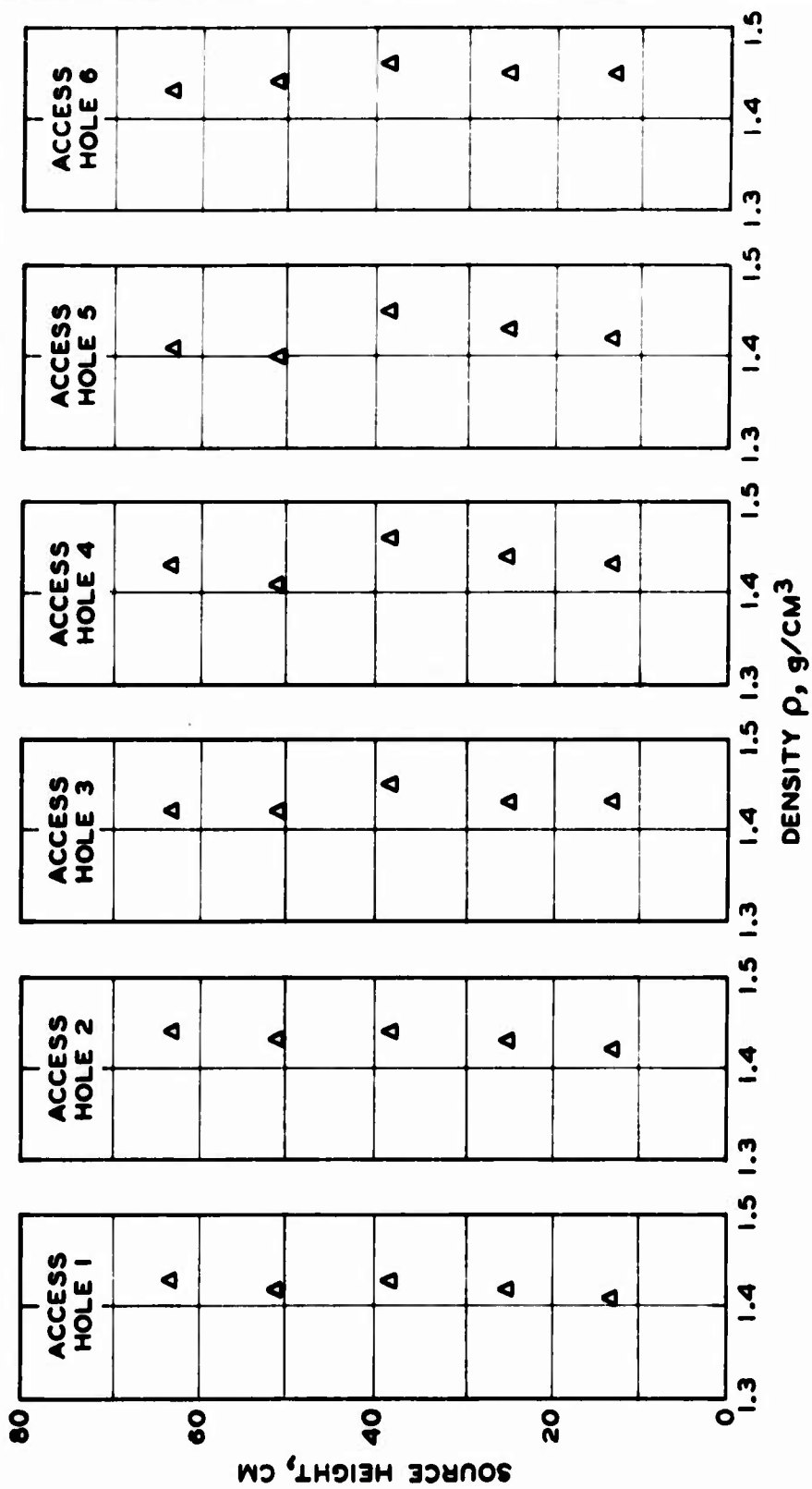
DENSITY VS SOURCE HEIGHT
YUMA SAND
MOISTURE CONTENT ≃ 0.5%
SAMPLE I, SAMPLE HEIGHT = 121.8 CM

PLATE I

DENSITY VS SOURCE HEIGHT
YUMA SAND
MOISTURE CONTENT ≈ 0.5%
SAMPLE 2, SAMPLE HEIGHT = 124.5 CM

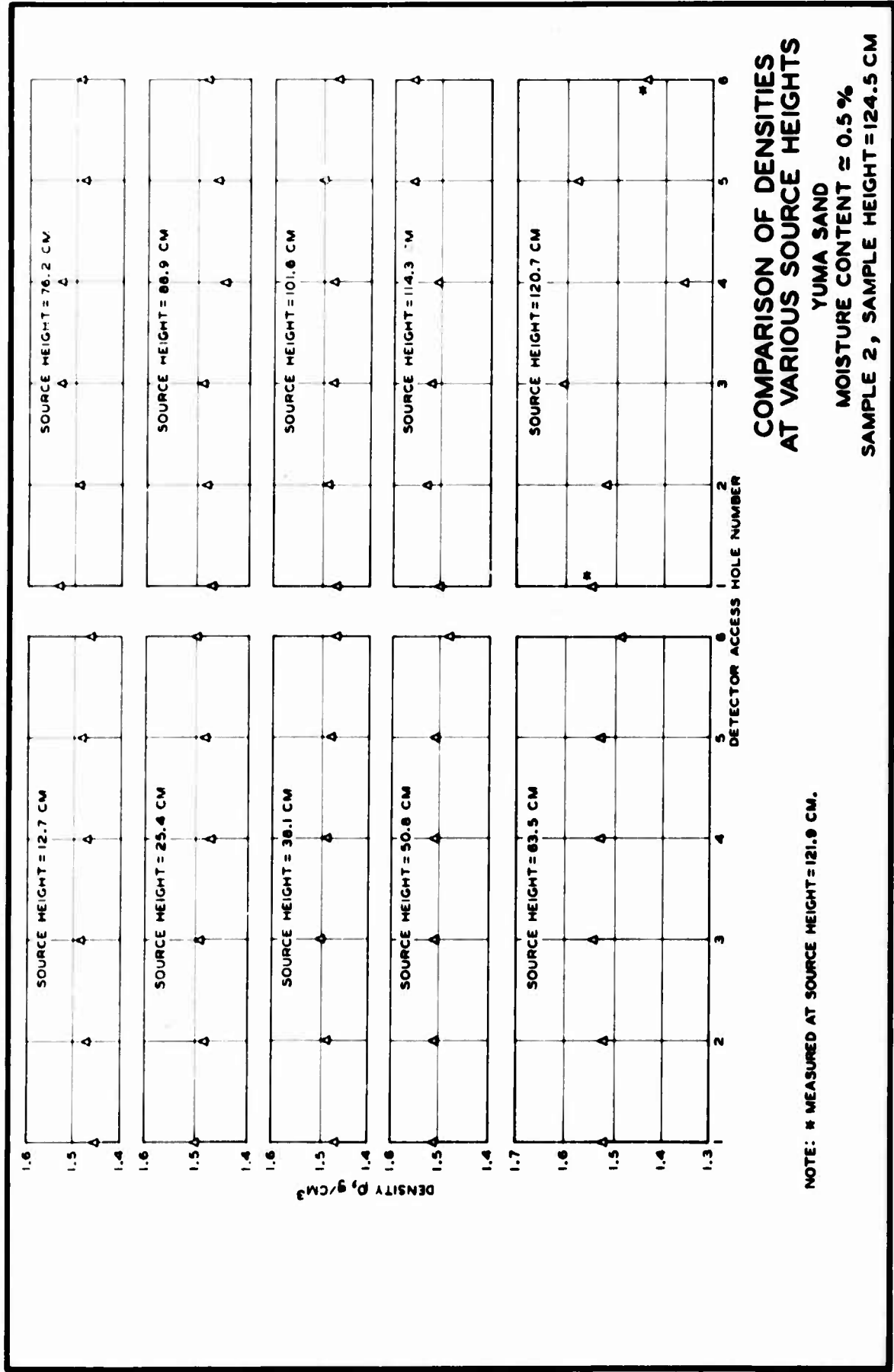PLATE 2

COMPARISON OF DENSITIES
AT VARIOUS SOURCE HEIGHTS
YUMA SAND
MOISTURE CONTENT ≃ 0.5 %
SAMPLE I, SAMPLE HEIGHT = 121.8 CM

PLATE 3

COMPARISON OF DENSITIES
AT VARIOUS SOURCE HEIGHTS
YUMA SAND
MOISTURE CONTENT ≃ 0.5%
SAMPLE 2, SAMPLE HEIGHT = 124.5 CM

NOTE: # MEASURED AT SOURCE HEIGHT = 121.9 CM.

PLATE 4

DOCUMENT CONTROL DATA - R & D

(Security classification of title, body of abstract and indexing annotation must be entered when the overall report is classified)

1. ORIGINATING ACTIVITY *(Corporate author)*	2a. REPORT SECURITY CLASSIFICATION
U. S. Army Engineer Waterways Experiment Station Vicksburg, Mississippi	Unclassified
	2b. GROUP

3. REPORT TITLE

PENETRATION RESISTANCE OF SOILS; Report 2, GAMMA-RAY TECHNIQUES FOR NONDESTRUCTIVE MEASUREMENTS OF SOIL DENSITY AND DENSITY PROFILE

4. DESCRIPTIVE NOTES *(Type of report and inclusive dates)*
Report 2 of a series

5. AUTHOR(S) *(First name, middle initial, last name)*

Albert N. Williamson, Jr.

6. REPORT DATE	7a. TOTAL NO. OF PAGES	7b. NO. OF REFS
November 1970	53	11

8a. CONTRACT OR GRANT NO.	9a. ORIGINATOR'S REPORT NUMBER(S)
b. PROJECT NO. 4A013001A91D	Technical Report M-70-14, Report 2
c. Item S	9b. OTHER REPORT NO(S) *(Any other numbers that may be assigned this report)*
d.	

10. DISTRIBUTION STATEMENT

This document has been approved for public release and sale; its distribution is unlimited.

11. SUPPLEMENTARY NOTES	12. SPONSORING MILITARY ACTIVITY
	Assistant Secretary of the Army (R&D) Department of the Army Washington, D. C.

13. ABSTRACT A study was conducted to determine the feasibility of using measurements made with a multichannel gamma-ray spectrometer and a cobalt 60 radiation source for accurately determining soil density and resolving the density profile of layers. Measurements were first made on aluminum and steel plates to establish a standard reference for comparing soil density. Two samples of air-dry sand were constructed at different densities to a depth of approximately 120 and 125 cm in a pit 51.82 m long and 3.54 m wide. Measurements were made at depth intervals of 12.7 cm in each of six access holes located in the samples. The densities determined were compared with densities determined by nonnuclear means. Results of this study indicate that density can be measured accurately by the method described herein provided (a) the thickness through which the measurements are made is accurately measured, and (b) the source strength and detector are suitable for the distance over which the density is measured. The combination of source and detector that was used permitted defining soil density profiles. As a result of this study, it is recommended that the method described herein be used for nondestructive soil density measurements where the density beneath the surface of a sample must be known.

DD FORM 1473 REPLACES DD FORM 1473, 1 JAN 64, WHICH IS OBSOLETE FOR ARMY USE.

14. KEY WORDS	LINK A		LINK B		LINK C	
	ROLE	WT	ROLE	WT	ROLE	WT
Gamma rays						
Nondestructive measurement						
Soil density						